Magnetic Field Stimulation of Bent Neurons

by
Mohammad Abdeen
Bachelor of Science in Engineering (Electronics & Communications), Egypt
Ain-Shams University, Cairo, 1989

A Thesis Submitted in Partial Fulfillment of the
Requirements for the Degree of

MASTER OF APPLIED SCIENCE
in the Department of
Electrical and Computer Engineering

We accept this thesis as conforming
to the required standard

Dr. M. A. Stuchly, Supervisor

Dr. J. Bornemann, Departmental Member

Dr. P. Fisher, Outside Member

Dr. D. Olesky, External Examiner

Supervisor: Dr. M. A. Stuchly

ABSTRACT

Magnetic neural stimulation of straight neurons with bends (1) in a semi-infinite volume conductor with a planar interface and (2) in the model of the human head is analyzed. Two stimulating coils, namely the double-square and the double circular, producing the magnetic field for the neuron stimulation are considered. The results indicate that the stimulating coil characteristics (size, shape and location) and the neuron shape affect the magnitude and location of the stimulation. The activating function, defined as the electric field derivative along the neuron, has two components. One component depends on the derivative of the electric field along the straight section of the neuron, and the other on the field magnitude. For bent neurons in a semi-infinite volume conductor, an analytical expression of the activating function (the stimulus) of the neuron was derived. The maximal stimulation point is at the bend of the nerve and its position depends on the nerve shape and coil parameters. The analysis also shows a better performance (a stronger stimulus) for a double-circular (figure eight) coil than for a double-square coil of comparable size.

Stimulating bent neurons in the human head is also analyzed. The head model consists of an outer sphere representing the skull and scalp and two inner spheres such that each represents one half of the brain. The 3D-impedance method was used to obtain the induced electric fields by the double-square and double-circular coils. Quasi-static conditions are assumed. The geometry of the neuron in this model approximates the normal configuration of motor neurons in the human head. The analysis shows that the stimulation occurs almost at the highest point on the nerve (the closest point to the coil) with the

coil positioned in such a way that its center is directly over the highest point on the nerve. It is also shown that the double-square coil produces a stronger stimulus than the double-circular coil. This result is in contradiction with that for a bent neuron in a semi-infinite volume conductor, however, it agrees with the results obtained for a straight neuron [1].

The analysis of bent neurons represents a more realistic approximation of the actual anatomy. The results of this analyses confirms the conclusions and, therefore, use-fulness of simplified analyses of straight neurons. The results are expected to be of some use in clinical applications where non-invasive neural stimulation is desired and location of stimulation needs to be known.

Examiners

Dr. M. A. Stuchly, Supervisor

Dr. J. Bornemann, Departmental Member

Dr. P. Fisher, Outside Member

Dr. D. Olesky, External Examiner

Table of Contents

List of Tables

List of Figures

Acknowledgments

I would like to express my deepest gratitude to my supervisor, Dr. M. A. Stuchly, for her continuous support and encouragement and for giving lots of her precious time to supervise this research work and the process of writing this manuscript.

I would like also to thank my colleague, Krzysztok Caputa, for helping me in checking the coil data used in this work as well as my colleague Ayman El-Sayed for stimulating useful discussions.

Finally, I express my full gratitude to all members of my family, especially my parents, for being with me with their hearts all the time.

Dedication

To My Parents

Chapter 1

Introduction

1.1 Background and motivation

Research in biomedical engineering is stimulated by an increasing interest in human health and by the tremendous progress in the technology of electronics, signal and image processing, computer control and applied electromagnetics.

Applications of the time-varying magnetic fields in medical research and clinical practice is one of the most active and promising areas in biomedical engineering. Time-varying magnetic fields are used as both diagnostic and therapeutic tools in medical applications. Diagnostic applications include magnetic stimulation [2], magnetic resonance imaging (MRI) and spectroscopy (MRS), and impedance (conductivity) measurements [3]. Therapeutic applications are in bone and other tissue repair and growth, energy transfer to implanted devices (electrical cardiac assist devices, biotelemetry, muscle and neural stimulators), hyperthermia and selective tissue destruction such as cardiac angioplasty and ablation, aneurysm treatment, and brain tumor resection [3]. Because the variety of applications have different requirements, a wide range of frequencies and magnetic field intensities are used.

In magnetic stimulation, short (micro- and millisecond range) but very intense current pulses are supplied to the stimulating coil to produce a fast rising strong magnetic

field to stimulate nerve fibers in the cerebral cortex or peripheral nerves. The pulses are repeated at low rates in the order of tens per second. This technique is clinically used to diagnose disorders in the nervous system. It is important to physicians when they stimulate a neuron using a magnetic field to know where to place the coil with respect to the nerve, and where, on the nerve, the stimulation takes place.

An ongoing challenge facing biomedical engineers is to develop the representative model of a bioengineering problem. A model is a limited representation of reality. It is something simple made by a scientist to help him understand a complicated problem. A model can consist of mathematical equations, an imaginary molecular structure obeying the laws of physics, or a machine which is physically different from the original phenomenon but which simulates its behavior. Modeling is usually a compromise between complexity and accuracy. A good model simulates the behavior of the modeled system within a small percentage error (e.g. 5%). The more accurate results it gives, the more involved the solution is. Developing a good model requires understanding of the nature of the problem so that the correct formulation is obtained and the suitable simplifying assumptions are made.

The role of engineers in the problem of magnetic neural stimulation are:

1- To model the neuron and its surrounding environment (the arm, the leg, or the head).

2- To solve for the important parameters, namely, the magnitude of the activating function (stimulus) and the location of the stimulation. The challenge in this step is to choose a suitable method of solution whether analytical or numerical.

3- To determine the best coil configuration and dimension (circular, square, double-square, etc). This step usually requires optimization, especially if the number of optimized variables is quite large.

1.2 Research objectives

In this thesis, we discuss one of the applications of the time-varying magnetic field in medical practice, namely the **magnetic neural stimulation.**

The objective of the research described is to model and analyze certain aspects of neural stimulation with magnetic fields, in order to better understand which parameters of stimulating coils and neuron geometry affect the efficiency of stimulation. Two aspects are analyzed:

- Bent neurons.
- The anatomical heterognaity of the human head.

Both aspects are of a special importance in the process of magnetic neuron stimulation in the human cortex.

The study of the first aspect will envolve examining the behaviour of the bent neuron in a simplified model, namely a semi-infinite volume conductor with a planar interface. Two parameters are examined, the magnitude of the activating function and the location of the stimulation. Determining the magnitude of the stimulation helps designers specify the suitable current values for the stimulating coil (to minimize the power consumption*), while determining the location of the stimulation allows physicians to determine the propagation time delay from the point of stimulation to the destination (e.g. a muscle) and thereby helps to diagnose any neuron disorder.

In the second aspect, the effect of the heterogeneous structure of the head on stimulation of bent neurons is analyzed. Considering the heterogeneous structure of the head gives more accurate stimulation parameters as well as a better understanding of the process of the neuron stimulation of the human cortex.

* Supplying high currents to the coils requires high capcaitor values. High capacitors are quite bulky and unpractical to use.

1.3 Thesis organization

To understand the technique of magnetic neural stimulation, how it is used as a diagnostic tool, and to study the different parameters affecting, it is necessary to acquire some basic knowledge of the anatomy of the nervous system as well as the anatomy of a single neuron. It is also important to have some background in neurophysiology to understand the mechanism that causes the neuron stimulation (action potential) and the mechanism of propagation of the signal in the nerve fiber. As we are only concerned with the engineering aspects of medical application, only a brief review of the anatomy of the nervous system and the neurobiology is presented in chapter 2. The chapter also contains discussion of the main engineering aspects of magnetic neural stimulation; its definition, the circuit model of the neuron, the technique of stimulating neurons and the coils and circuitry used.

Determining the location as well as the value of the maximum activating function (the stimulus) are the goals of solving a problem of magnetic neural stimulation. Most of the problems discussed in previous work considered the value and location of the stimulus for *long straight* axons [1]. In chapter 3, the computation of the induced electric fields, as well as the activating function of the neuron during the process of magnetic stimulation are described. Also, a review of previous work in the area of magnetic neuron stimulation is presented. In this review, different models of neuron stimulation, as well as the different methods of solution and results are highlighted. The models discussed are: (1) a long straight neuron in a semi-infinite volume conductor with a planar interface, (2) a long straight nerves in a cylindrical volume conductor (this model is suitable when stimulating peripheral neurons in the arm or the leg), and (3) neurons in a spherical volume conductor. The latter is a good model when studying the neuron stimulation of the human cortex.

Except for an experimental work done by Maccabee et al. [4], no theoretical study

has been done to calculate the value of the activating function and location of the stimulation for straight neurons with bends. Such analysis may be relevant to nerves entering fissures of the cerebral cortex. The goal of the discussion in chapter 4 is to develop a theoretical model for straight neurons with bends in a semi-infinite volume conductor. In this analysis, three different bends are considered; circular, parabolic and hyperbolic cosine. For long straight axons it is well established that the activating function is the spatial derivative of the electric field [5],[6]. On the other hand, for straight neurons with bends, the activating function depends on both the spatial derivative of the electric field as well as the electric field itself. The analysis is done for two different coil shapes that are commonly used in magnetic neural stimulation, namely, the double-square and the double-circular coils.

The technique of magnetic stimulation is not restricted to stimulating peripheral nerves that are modeled as long straight nerves in a semi-infinite or cylindrical volume conductors, but it is also used to activate neurons in the cortex [7], map the motor cortex [8], and in central motor conduction studies [9]. Several investigations have modeled the induced electric field in the brain during magnetic stimulation. Some models have neglected the conductor boundary [10], while others have treated it as an infinite conducting half space [11]. More advanced models include a quasi-spherical volume analyzed with finite-element techniques [12] and a layered sphere model, corresponding to the human head layers skull, scalp, and cortex, using a finite-difference technique [13]. An analytical model for magnetic stimulation of the human head has also been developed by Eaton [14]. In all of the previous models, it has been shown that the radial component of the electric field is either zero or highly attenuated [13],[14] and accordingly, radial neurons can not be stimulated. These models are not really exact models of the human head, specially the inner most sphere which models the cortex. The cortex is actually consists of two parts and a better model consists of two eccentric spheres as considered in this

work. In chapter 5, the eccentric spheres model of the human head is studied. The model takes into account the heterogeneous structure of the head by assigning two different conductivities for the two spheres representing the brain and the outer sphere representing the skull and scalp. The activating function as well as the location of the stimulation are obtained for the two coil configurations commonly used, namely the double-square and the double circular coils. The analysis shows that the magnitude of the activating function depends on both the coil configuration and the bend shape in agreement with the case of semi-infinite volume conductor.

Finally, the general conclusions and future work are presented in chapter 6.

Chapter 2

Neural stimulation

2.1 Introduction

Ever since the work of Galvani and Volta in the 1790's, it has been known that nerves and muscles can be electrically stimulated. Stimulation of a nerve produces an electrical pulse (action potential) which propagates along it. Electrical stimulation can be achieved by an electric field having a non-zero spatial derivative in the direction of the nerve. The technique of electrical nerve stimulation using either needle or surface electrodes is widespread today for diagnostic and therapeutic purposes. More specifically, nerve stimulation has been recognized as a diagnostic tool for brain/spinal cord disorders e.g. multiple scelerosis, visual perception problems, cerebral palsy, and facial paralysis [3]. Magnetic stimulation is another way of achieving the same effect, of inducing electrical current in the tissue to cause nerve stimulation. Magnetic stimulation offers the advantage that it is a non-contact and non-invasive method which produces minimal discomfort to the patient as only low density current flows through skin pain receptors during the procedure.

2.2 Physiology of the nerve fiber

2.2.1 The nervous system

The survival of any multicellular organism depends on some means of regulating and coordinating the activities of its cells. The human organism has two systems that serve as

the means of internal communication among the organs: the nervous system and the endocrine system.

Structurally, the nervous system may be divided into two parts: the central nervous system and the peripheral nervous system. The central nervous system (CNS) consists of the brain and the spinal cord [15]. It is completely encased in bony structures - the brain within the cranial cavity of the skull and the spinal cord within the vertebral canal of the spinal column. The central nervous system is the integrative and control center of the nervous system. It receives sensory input from the peripheral nervous system and formulates responses to this input.

The peripheral nervous system (PNS) is composed of all nerve structures located outside of the central nervous system. Specifically:

1. Nerves that connect the outlying parts of the body and their receptors with the central nervous system.

2. Ganglia (groups of nerve cell bodies) associated with the nerves.

In our study we will consider only the first category of the PNS, namely the nerves.

2.2.2 Structure of the nerve cell

The nerve cell (neuron) is the basic structure and functional component of the nervous system. It responds to stimulation by initiating and conducting electrical signals. Some other cells, such as muscle fibers, are also capable of conducting electrical signals, but the unique shape of the nerve cell makes it especially well suited to serve as a communicator.

Each neuron is composed of a cell body (soma) and one or more processes that extend from the cell body (each cell contains cytoplasm, Fig. 2.1) [15]. The processes associated with a neuron are very thin extensions of the cell. There are two types of processes: dendrites and axons. The dendrites conduct signals toward the cell body (receptive portion of the neuron); axons conduct electrical signals away from the cell body (transmittive portion of the neuron).

There is a considerable variation in the size of nerve cells. The diameters of vertebrate neurons range downward in size from approximately 30 microns to just a few microns. It is difficult to estimate the length of the dendrites; however, they probably reach a maximum of 2 mm in the outer layers of the cerebral cortex. Axon lengths vary from a minimum in the order of 50 microns to a maximum of several meters in large mammals [15].

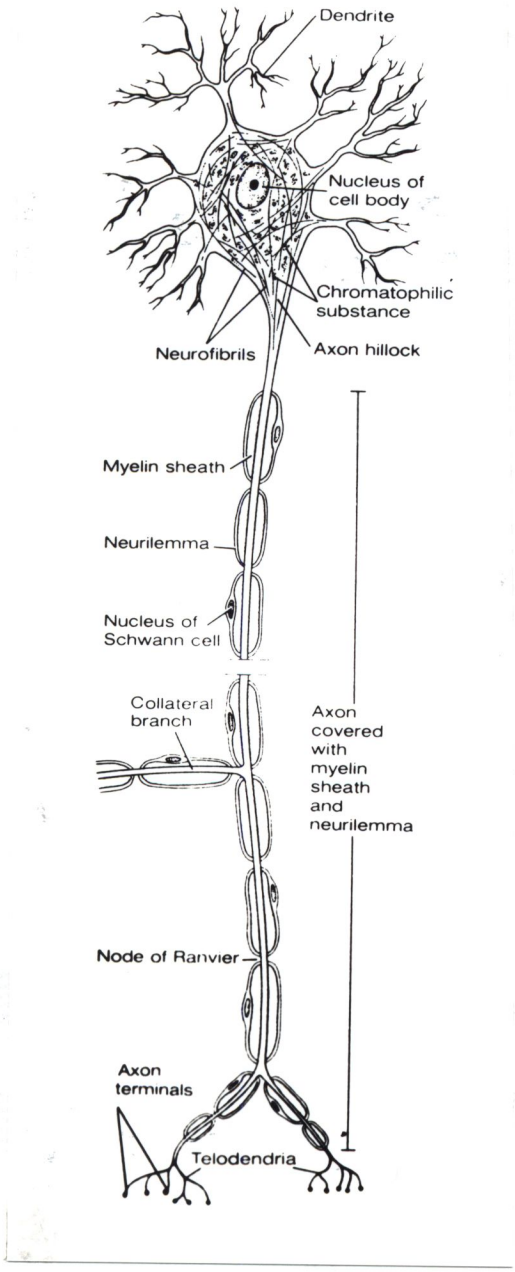

Figure 2.1 Structure of a typical motor neuron

Large nerve fibers are surrounded by a myelin sheath of mainly lipoid material, as shown in Fig. 2.2-a . The sheath is regularly interrupted at axial intervals of about 1mm to give pronounced indentations known as nodes of Ranvier as shown in Fig. 2.2-b [16].

(a)

(b)

Figure 2.2 Myelinated nerve fiber. (a) A cross section normal to the neuron axis. (b) A longitudinal cross section showing nodes of Ranvier.

Neurons can be classified according to their function into three types [15]:

1. Motor neurons, which transmit impulses away from the CNS to an effector (a muscle).

2. Sensory neurons, which carry impulses from receptors to the CNS.

3. Interneurons, which, when present, transmit impulses from one neuron to another.

The modeling presented in this thesis concerns motor neurons.

2.2.3 The cellular membrane

The functional boundary of the cell is a thin (about 8-nm) lipid bilayer with embedded proteins layer [17]. The membrane regulates ion concentration gradient between the area inside the cell (the plasm) and the area outside the cell (the interstitial fluid). The cytoplasmic and interstitial fluids are composed largely of water containing different ions. The difference in concentration of ions causes electrochemical forces across the cell membrane. The membrane, which is semipermeable, is basically a dielectric insulator that allows some ionic interchange. Fig. 2.3 represents the membrane as a barrier with pores that permit the passage of ions. The individual pores may be very selective of the ions they allow to pass. Although other types of ions are also present, only the Na, K, and Cl ions will be considered as they are sufficient for our purpose [17].

2.2.4 The neuron at rest

Fig. 2.3 also shows the membrane and the outer and inner ionic concentrations of various ions mentioned above [17]. The differences in these concentrations result in two forces that tend to drive ions across the membrane: a concentration gradient and a voltage gradient. Due to both, concentration gradient and semi-permeability of the neuron cell, a volt-

age difference is built up across the cell membrane until equilibrium is reached. The membrane voltage at equilibrium conditions is known as the membrane resting potential and is given by [18]:

$$V_m = \frac{RT}{F}\log\left(\frac{[K]_e + \alpha[Na]_e}{[K]_i + \alpha[Na]_i}\right) \tag{2.1}$$

where

$$\alpha = \frac{P_{Na}}{P_K} \tag{2.2}$$

and P_{Na} and P_K (cm/s) are the membrane permeability to sodium and potassium, respectively, R is the universal gas constant (8.31 J/mol K), T is the absolute temperature (310 K), F is the Faraday constant (96,500 C/mol), $[K]_{e,i}$ and $[Na]_{e,i}$ are the concentrations of the potassium and sodium outside and inside the membrane, respectively. At resting conditions the membrane potential is around -70 mV.

Equation (2.1) is known as Nernst equation for potassium and sodium.

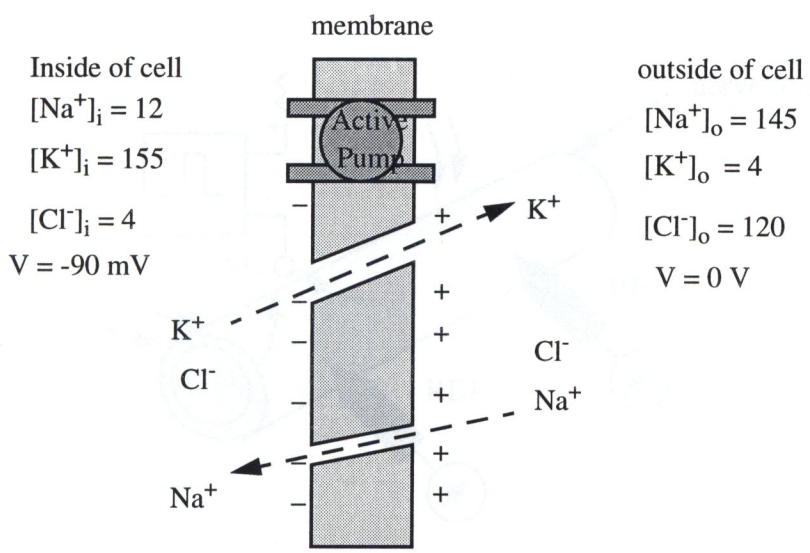

Figure 2.3 Chemical composition of a typical cell membrane

2.2.5 The excitable membrane

To illustrate the properties of the excitability and propagation, consider the experiment illustrated in Fig. 2.4 in which a small stimulating electrode (SE) is near a nerve fiber and two small recording electrodes (RE) pierce the membrane. The voltage disturbance caused by the SE will tend to decrease the negativity of the membrane potential (depolarization) near the cathode and increase its negativity (hyperpolarization) everywhere else along the axon [17]. Fig. 2.5 illustrates the response of the membrane to rectangular current pulses shown in the upper part of the figure [17]. Six possible current magnitudes, labeled *a* through *f*, are shown. Pulses *a* through *c* correspond to an anode as the SE; pulses *d* through *f* correspond to a cathode as the SE. The membrane response is shown as measured by RE1 and RE2, where 0 mV represents the resting potential. Responses *a* through *c* are in the direction of hyperpolarization, and responses *d* through *f* are in the direction of depolarization. From the circuit theory point of view responses *a* though *f* can be described by two different models.

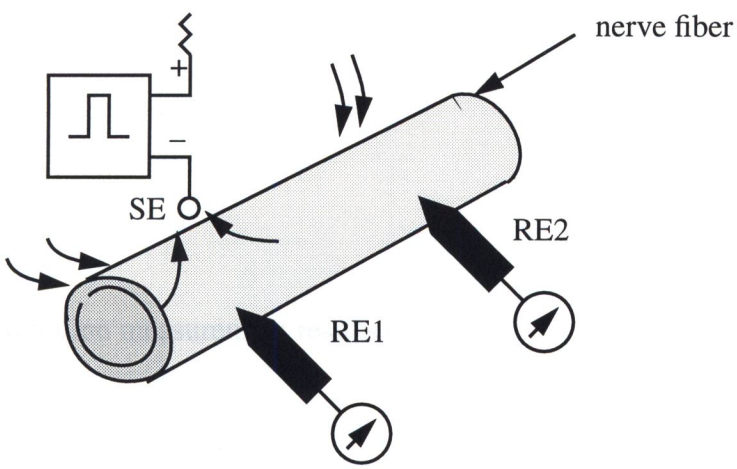

Figure 2.4 Nerve excitation setup

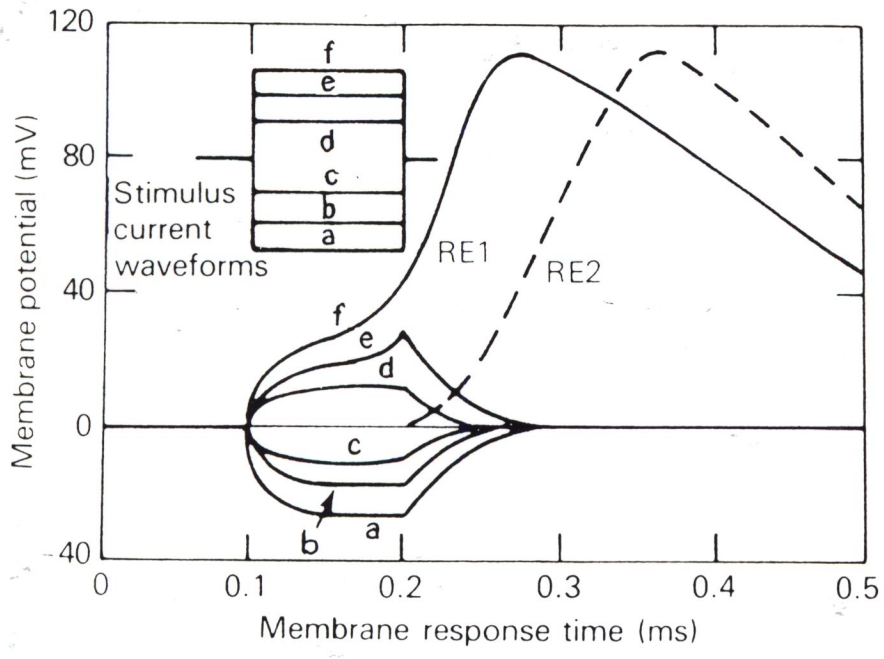

Figure 2.5 Nerve excitation measurement results

1- Passive cable model [19]

Responses *a* through *d* (correspond to subthreshold stimulus) exhibit the characteristic of a linear network consisting of a parallel combination of a resistor and a capacitor. Fig. 2.6 shows the circuit model of the nerve corresponding to its linear behavior (responses *a* through *d*). The model is called the Passive Model. In this model, r_i is the intracellular resistance per unit length, r_m is the membrane resistance times length, c_m is the membrane capacitance per unit length and Δx is the nodal distance for myelinated fiber ($\Delta x \rightarrow dx$ for unmyelinated fibers). The membrane potential is obtained by applying Kirchhoff's current law at the n^{th} segment of the nerve (marked by a black circle in Fig. 2.6), that is $\Sigma I = 0$. We get [20]

$$\frac{dV_n}{dt} = \left\{ \frac{d}{4\rho_i} \cdot \left(\frac{V_{n-1} - 2V_n + V_{n+1}}{\Delta x \cdot L} + \frac{V_{e,n-1} - 2V_{e,n} + V_{e,n+1}}{\Delta x \cdot L} \right) - J_{ion,n} \right\} / c_m \qquad (2.3)$$

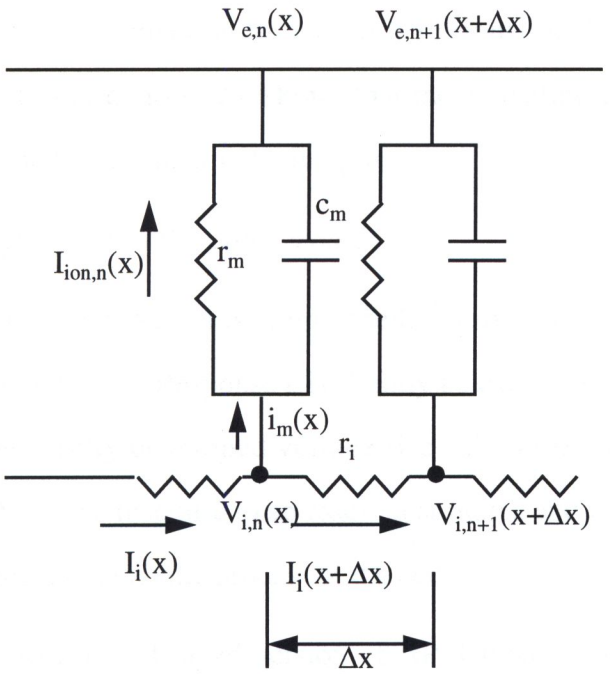

Figure 2.6 Passive cable model of cellular membrane

where d is the fiber diameter (m), r_i is the resistivity of the axoplasm, L is the active length of the membrane, $J_{ion,n}$ is the total ionic current density (A/m^2), c_m is the membrane capacitance per meter square (F/m^2), L is the nodal gap width and Δx is the internodal length for myelinated fiber. V_n is then defined as:

$$V_n = V_{i,n} - V_{e,n} + V_{rest} \tag{2.4}$$

where $V_{e,n}$ and $V_{i,n}$ are the external and internal potentials of the n^{th} segment.

If we define $f_n(t)$ as:

$$f_n(t) = \frac{V_{e,n-1} - 2V_{e,n} + V_{e,n+1}}{\Delta x \cdot L} \tag{2.5}$$

then, as Δx tends to zero (unmyelinated fiber), $f_n(t)$ reduces to $f(x,t)$, where

$$f(x,t) = \frac{\partial^2}{\partial x^2} V_e(x,t) \tag{2.6}$$

$f(x,t)$ is called the activating function because it is responsible for activating a fiber by extracellular stimulation. Equation 2.6 shows that the activating function is the second spatial derivative of the extracellular potential [20].

2- Action potential and active cable model

As a critical level of depolarization is approached, approximately 20 mV (in Fig. 2.5), nonlinear behavior is observed. Response e is slightly below the excitation threshold, and response f illustrates a fully developed voltage rise called the Action Potential (AP). Action potential is the nerve response to an external stimulus and is caused by the release of energy accumulated by metabolic process of the cell.

The signal at RE2 is a delayed version of AP demonstrating propagation of AP along the axon. The membrane response is often referred to as "all-or-none" because the peak of the AP is not affected by the magnitude of the current pulse once it exceeds

threshold [17]. This nonlinear behavior of the neuron is represented in the circuit model by nonlinear conductances, instead of linear resistance in the passive cable model. The circuit model of the excitable membrane (shown in Fig. 2.7) was developed by Hodgkin and Huxley and is named after them.

For an excited membrane, the total ionic membrane current density $J_{ion,n}$ in equation (2.3) has to be modified so that the ionic currents of sodium and potassium are taken into account. The membrane current is given by:

$$J_{ion} = J_{Na} + J_K + J_L = g_{Na}(V - E_{Na}) + g_K(V - E_K) + g_L(V - E_L) \tag{2.7}$$

where g_{Na}, g_K and g_L are the ionic sodium, potassium and leakage conductances, respectively, and E_{Na}, E_K and E_L are the respective equilibrium potentials.

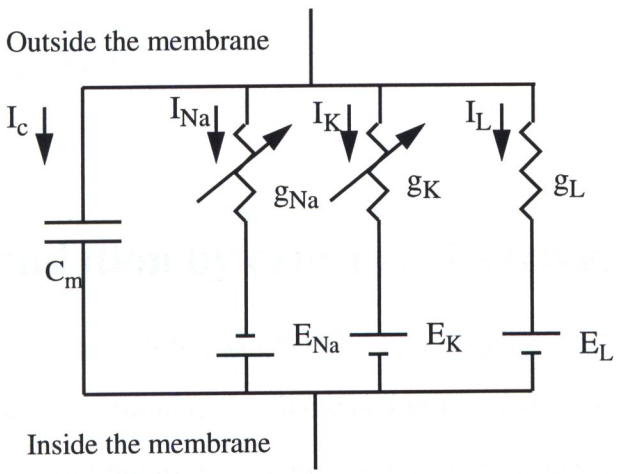

Figure 2.7 Excited membrane (Hodgkin Huxley) model

The g_L conductance is linear; the other two conductances are more complex nonlinear functions of the form [17]:

$$g_{Na} = \bar{g}_{Na} m^3 h \tag{2.8}$$

and

$$g_K = \bar{g}_K n^4 \tag{2.9}$$

where g_{Na} and g_K represent the maximum conductance values; and n, m and h are so-called activation and deactivation variables that modulate the maximum conductances[17].

The transmembrane potential for the excited membrane is obtained by simple substitution of equation (2.7) into equation (2.3).

$$\frac{dV_n}{dt} = \frac{1}{c_m} \cdot \frac{d}{4\rho_i}\left(\frac{V_{n-1} - 2V_n + V_{n+1}}{\Delta x \cdot L} + \frac{V_{e,n-1} - 2V_{e,n} + V_{e,n+1}}{\Delta x \cdot L} \right)$$

$$-\frac{1}{c_m} \cdot \left(J_{Na} + J_K + J_L \right) \tag{2.10}$$

2.3 Neuron stimulation by external electrodes

Before the 1980's, nerve stimulation was obtained by applying external or implanted electrodes near the nerve to be stimulated as indicated in Fig. 2.8 [21],[22]. A very high voltage pulse lasting for a brief duration is applied to those electrodes (e.g., a 2 kV pulse with a decay time constant of 10 μs) causing a current pulse to flow through the neuron. The regions where the current leaves the membrane are depolarized (point 1 in Fig. 2.8), while other regions in which current enters the membrane(point 2 in Fig. 2.8) are hyperpolarized. For external electrodes very high voltage pulses are used to force current

through a high resistance tissue (e.g. fat and bones in brain cortex neuron stimulation). The resulting high current pulse that stimulate pain receptors. Neuron stimulation by contact electrodes is an invasive process (for implanted or inserted electrodes).

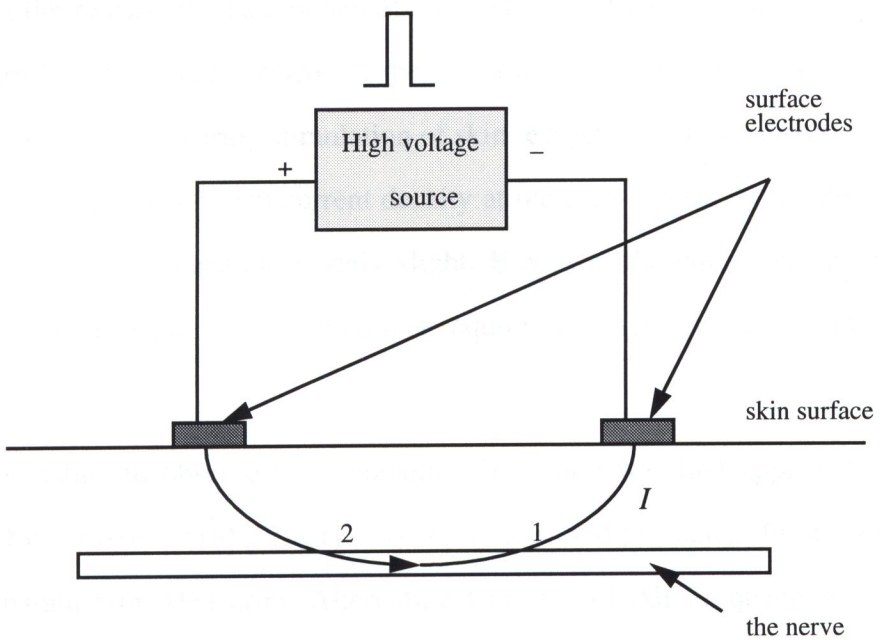

Figure 2.8 Nerve stimulation by external electrodes

2.4 Magnetic stimulation

Magnetic stimulation of a central nervous system is a painless alternative to electrical stimulation and is finding increasing use. The basic principle in magnetic stimulation is to make use of currents induced in a tissue when exposed to a time-varying magnetic field produced by a coil carrying a time-varying current (according to Faraday's law).

Magnetic (eddy-current) stimulation is increasingly used as a diagnostic and research tool following the clinical demonstration of peripheral nerve stimulation [23] and stimulation of the human brain [24]. The considerable advantage of magnetic-pulse stimulation is the remarkable lack of sensation when compared to stimulation with skin-surface electrodes. With such electrodes, there is a high current density under the electrode perimeter, thereby favoring stimulation of skin receptors. With magnetic pulse stimulation, there is no localized high current density at the skin surface under the excitation coil; therefore, the skin sensation is only slight. However, the equipment needed with magnetic stimulation is much larger than that required for skin surface stimulating electrodes.

It is interesting to observe that magnetic stimulation was first applied to the nervous system by d'Arsonal (1851-1941) [25], a physicist and physician. In his 1896 paper entitled "Apparatus for Measuring Alternating Currents of All Frequencies" he stated that an alternating magnetic field with an intensity of 110 volts, 30 amperes with a frequency of 42 cycles per second, give rise to, when one places the head into the coil, phosphenes and vertigo, and in some persons, syncope.

Kolin et al. (1959)[26] demonstrated, for the first time, that an alternating magnetic field could stimulate a nerve. They looped a frog sciatic-nerve-gastrocnemius-muscle preparation around the insulated pole face of an electromagnet. An intense contraction of the gastrocnemius muscle was obtained with 60 and 1,000 Hz current applied to the coil.

The muscle contraction was recorded and the rectified voltage picked up by a loop of wire around the pole face. To complete the investigation, the nerve-muscle preparation was placed in a Petri dish filled with saline. The dish was placed on the pole face, and alternating current was applied to the coil, resulting in a tetanic muscle contraction.This experiment offered conclusive experimental proof that a magnetic field could induce enough current in a volume conductor to stimulate a motor nerve.

The modern use of magnetic stimulation was introduced by Bickford et al. in 1965 [27], who caused skeletal muscle to twitch in intact rabbits, frogs, and human subjects by using a pulsed magnetic field. The pulse duration was about 300 ms, and the peak field strength was 2-3 T. They concluded by stating "The findings in both man and animals are consistent with the hypothesis that stimulation results from eddy currents induced in the vicinity of motor nerves."

2.5 Magnetic stimulator

A typical magnetic stimulator consists of a capacitor C which is charged to a voltage V_0 and then discharged through the stimulating coil of inductance L, and a resistance R as shown in Fig. 2.9. This stimulator produces a peak current of several thousand amperes during a pulse of a brief duration (typically 100 A/μs) [19]. Depending on the values of the stimulating circuit components (i.e. R, L, and C) the current either rises to a maximum

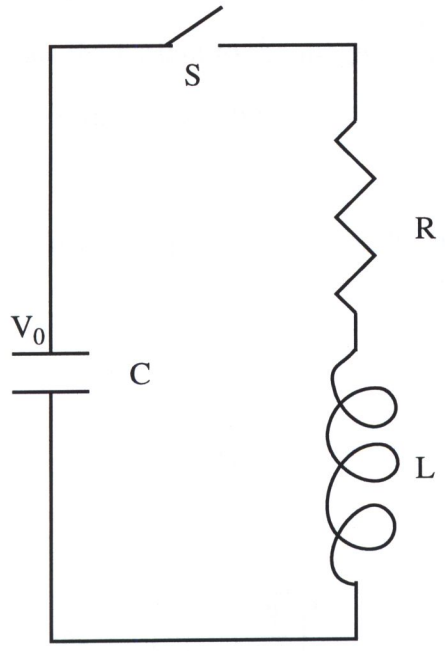

Figure 2.9 Typical magnetic stimulator

and then falls to zero (overdamped), or else it oscillates with decreasing amplitude (underdamped), depending whether $\left(R^2/4L^2\right) - (1/LC)$ is greater than or less than zero, respectively. The critically damped case $\left(R^2/4L^2\right) - (1/LC) = 0$ is difficult to achieve experimentally and will not be considered here. On the other hand, underdamped circuit is undesirable because, first, the waveform of the current will be oscillatory and its time derivative $\partial I/\partial t$ will have positive as well as negative values. The problem with the negative values of $\partial I/\partial t$ is that they will cause a depolarization of the nerve and thereby blocking the propagating action potential. Another problem associated with the secondary positive cycles of $\partial I/\partial t$ is that they might cause neural stimulation, and thus

we will not be able to know which cycle is responsible for the neuron stimulation. Also, the use of such circuit exposes the patient to the magnetic field for longer time. For an underdamped current, the waveform is given by:

$$I(t) = V_0 C \omega_2 e^{-\omega_1 t}\left(\left(\frac{\omega_1}{\omega_2}\right)^2 + 1\right) \cdot \sinh(\omega_2 t) \tag{2.11}$$

where

$$\omega_1 = \frac{R}{2L} \tag{2.12}$$

and

$$\omega_2 = \sqrt{\frac{1}{LC} - \left(\frac{R}{2L}\right)^2} \tag{2.13}$$

For an overdamped circuit, there is still a bi-phasic response of $\partial I/\partial t$. However, the magnitude of the negative phase part is small and controllable. The current in the coil for an overdamped response is given by:

$$I(t) = V_0 C \omega_2 e^{-\omega_1 t}\left(\left(\frac{\omega_1}{\omega_2}\right)^2 - 1\right) \cdot \sinh(\omega_2 t) \tag{2.14}$$

where ω_1 is the same as given above and

$$\omega_2 = \sqrt{\left(\frac{R}{2L}\right)^2 - \frac{1}{LC}} \tag{2.15}$$

For example, a circular coil of radius 2.5 cm with 30 turns wound from 1.0 mm radius wire has an inductance of 0.165 mH [19]. Assuming that C = 200 μF and R = 3.0 Ω, it can be found that the circuit is overdamped. The resulting current waveform and its time derivative are shown in Fig. 2.10 ,with V_0 = 200 Volts.

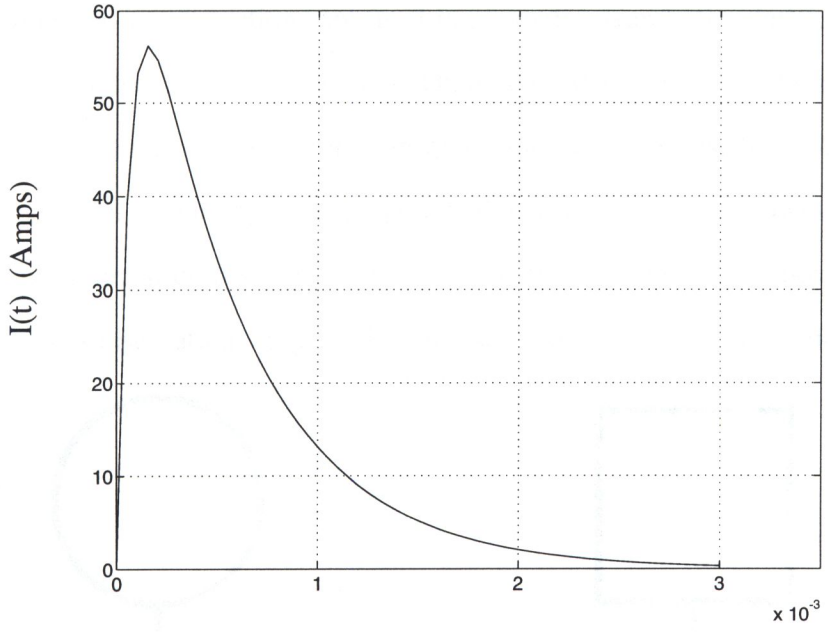

(a)

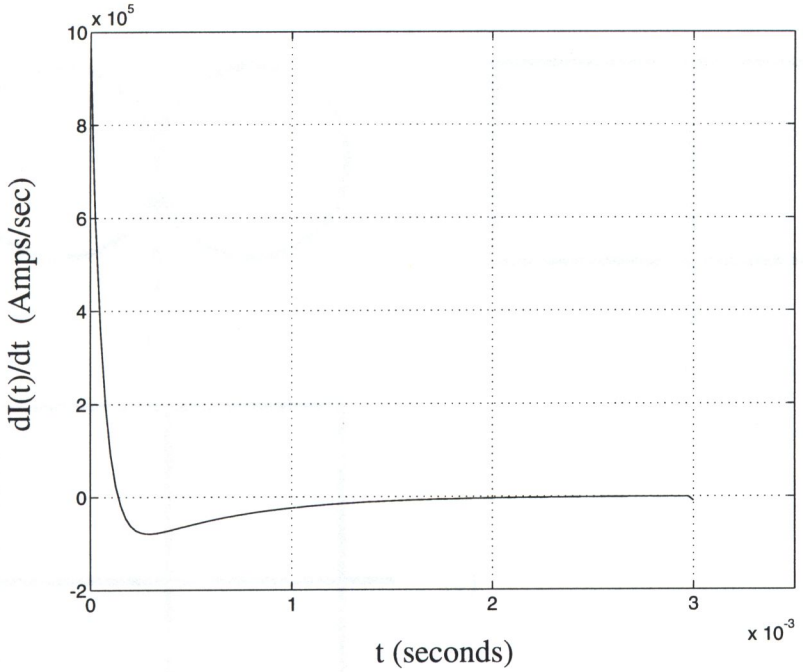

(b)

Figure 2.10 The time course of (a) the current stimulus I(t) and (b) its time derivative. This waveform was generated using (2.14), with R = 3 Ω, L = 0.165 mH, and C = 200 μF.

Different coil configurations are used in magnetic neural stimulation. Circular coils are simple and have been used widely. Other configurations include square, double-square, double-circular (figure eight) and quadruple-square coils. Stimulating coils can be oriented parallel, at an angle, or perpendicular to the interface, however, the parallel orientation is the most commonly used as coils with this orientation show better performance than other orientations. Fig. 2.11 shows some of the coil configurations used.

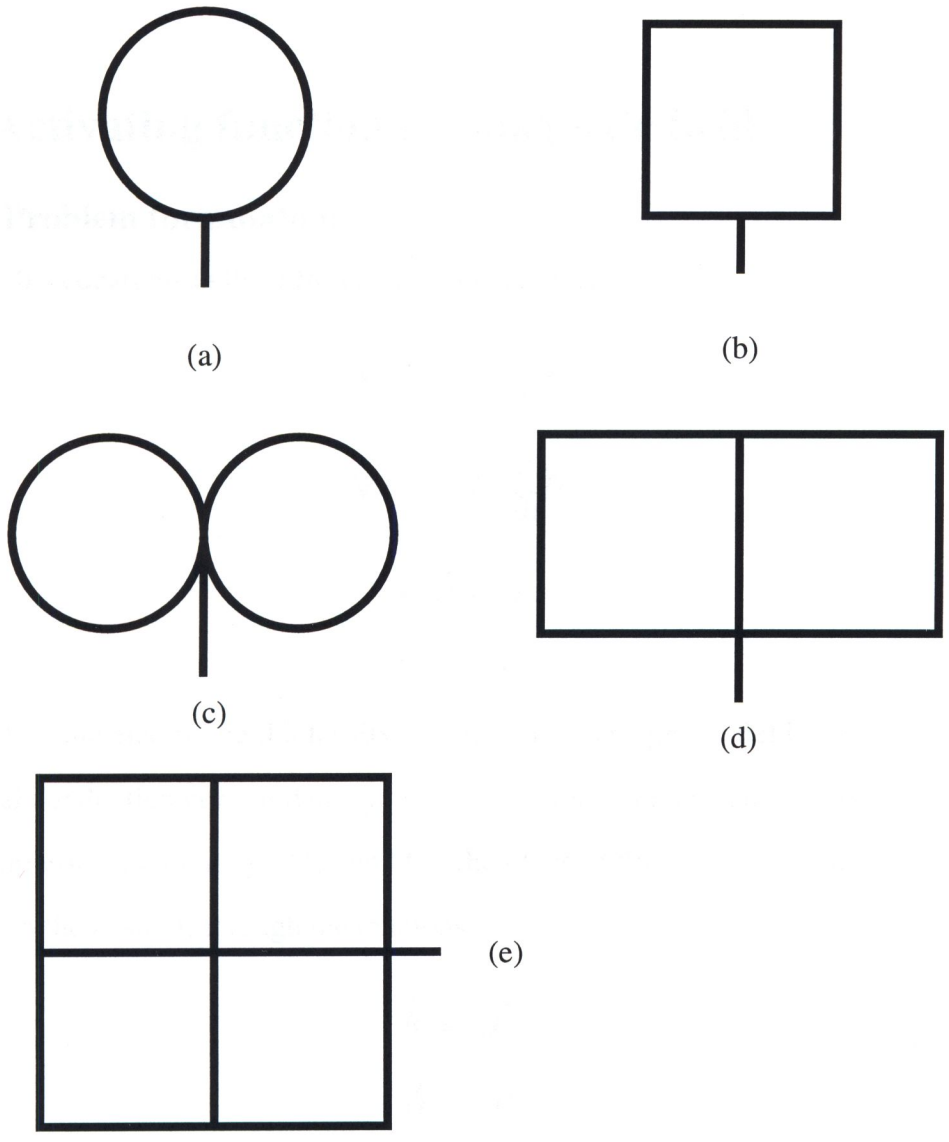

Figure 2.11 Different coil configurations (a) a circular coil (b) a square coil (c) a double-circular coil (d) a double-square coil (e) a quadruple-square coil.

Chapter 3

The state of knowledge

3.1 Activating function for magnetic field

3.1.1 Problem formulation

Maxwell's equations in the differential form are given by:

$$\nabla \times \vec{E} = -\frac{\partial}{\partial t}\vec{B} \tag{3.1}$$

$$\nabla \times \vec{H} = \vec{J} + \frac{\partial}{\partial t}\vec{D} \tag{3.2}$$

$$\nabla \bullet \vec{D} = \rho \tag{3.3}$$

$$\nabla \bullet \vec{B} = 0 \tag{3.4}$$

where E is the electric field intensity (V/m), H is the magnetic field intensity (A/m), J is the total conduction current density (A/m^2), ρ is the volume charge density (C/m^3), B is the magnetic flux density (T), and D is the electric flux density (C/m^2). B and D are related to the H and E through the relations:

$$\vec{B} = \mu\vec{H} \tag{3.5}$$

$$\vec{D} = \varepsilon\vec{E} \tag{3.6}$$

where μ is the permeability (H/m), and ε is the permittivity (F/m) of the medium.

In any electromagnetic problem, electromagnetic fields can be obtained by solving

the four Maxwell's equations (3.1) to (3.4). However, a simpler method is to formulate the Maxwell's equations in terms of scalar and vector potentials. As a consequence of (3.4) we can express the magnetic field as a curl of another vector A as:

$$\vec{B} = \nabla \times \vec{A} \tag{3.7}$$

where $\vec{A}$ is defined as the magnetic vector potential. Substituting (3.7) into (3.1) we obtain:

$$\nabla \times \left(\vec{E} + \frac{\partial}{\partial t} \vec{A} \right) = 0 \tag{3.8}$$

comparing (3.8) with the vector identity

$$\nabla \times (\nabla V) = 0 \tag{3.9}$$

where V is a scalar function, and as a corollary, any vector function with no curl is the gradient of some scalar function. Therefore, we can write:

$$-\nabla V = \vec{E} + \frac{\partial}{\partial t} \vec{A} \tag{3.10}$$

Obtaining the electric field from (3.10), then we have:

$$\vec{E} = -\frac{\partial}{\partial t} \vec{A} - \nabla V \tag{3.11}$$

where V is the scalar potential. In terms of the scalar and vector potentials, (3.2) and (3.3) become [28]:

$$\nabla^2 \vec{A} - \frac{1}{c^2} \frac{\partial^2}{\partial t^2} \vec{A} = -\mu \vec{J} \tag{3.12}$$

$$\nabla^2 V - \frac{1}{c^2} \frac{\partial^2 V}{\partial t^2} = -\frac{\rho}{\varepsilon} \tag{3.13}$$

where c is the speed of light in free space (m/s). Relations (3.12) and (3.13) are valid provided that A and V satisfy the Lorenz condition:

$$\nabla \bullet \vec{A} + \frac{1}{c^2}\frac{\partial V}{\partial t} = 0 \tag{3.14}$$

3.1.2 The quasi-static approximation

The calculation of the electric field induced in a tissue by a time-varying magnetic field is not new [29]. Such calculations have been performed in studies of hyperthermia treatment for cancer, where a radio-frequency magnetic field induces current in tissue, and the currents in turn heat the tumor [30]-[32]. While these studies have not specifically addressed magnetic stimulation, the theory and methods underlying these studies are generally applicable.

When calculating the electric field induced in biological tissues during magnetic stimulation, three assumptions are made leading to the "quasi-static", or low frequency, approximation [33]. First, the wavelength of electromagnetic waves is much less than the largest dimension of the geometry under consideration, l. At the frequencies of interest in magnetic stimulation, up to 10 kHz, the wavelength of the electromagnetic radiation is $\lambda \approx 100$ m. This value can be obtained from a typical value of relative permittivity ε_r of biological tissues of 10^5 [34]. The wavelength is much longer than any distance associated with the human body. This assumption ($l/\lambda \ll 1$) leads to the conclusion that effects associated with the finite velocity of propagation of electromagnetic waves may be neglected. Mathematically, this is equivalent to dropping the displacement current term, $\partial\vec{D}/\partial t$, from Maxwell's equation (3.2). This is called the quasi-static approximation [28]. Only at frequencies of 30 MHz and higher it is necessary to include the finite wave length into account in bioelectric calculations [35]-[37], although recently a complex calculation was performed that considered the finite wavelength in a study of currents induced during magnetic stimulation [38].

A second approximation is to neglect the skin depth, the distance which electromagnetic fields can penetrate into tissue. An external time-varying magnetic field causes current to flow in tissue by electromagnetic induction. These currents induced in the tissue produce their own magnetic field that tends to cancel out the applied field, and this cancellation becomes more complete with depth into the tissue. The depth at which the magnetic field in the tissue is $1/e$ of the external field is called the skin depth, δ. It depends on the frequency, f, the conductivity, σ, and magnetic permeability, μ, of the tissue. The skin depth is given by:

$$\delta = \sqrt{\frac{1}{\mu\pi\sigma f}} \tag{3.15}$$

Almost all biological tissues have a permeability equal to that of air, μ_0 ($4\pi \times 10^{-7}$ H/m), the conductivity of tissue is typically on the order of 1 S/m [39], and the highest frequency of interest is approximately 10 kHz (corresponding to a 100 μs rise time of the current pulse), yielding a skin depth of 5 meters. This depth is large compared to the dimensions of the human body. Thus, skin depth can be neglected in these calculations, which is equivalent to saying that the magnetic field produced by the current in the tissue is small compared to that produced by the current in the coil.

The third approximation is to neglect capacitive effects. The impedance of a multicellular tissue can be modeled by combinations of resistors and capacitors, where the resistors represent the intracellular and interstitial spaces and the capacitors represent the cell membranes [39]. These circuit elements can be combined to yield an overall tissue impedance containing resistive and capacitive terms. The ratio of the capacitive and resistive terms is the ratio of the displacement to the conduction currents density, $\left(\frac{\partial}{\partial t}\vec{D}\right)/\sigma\vec{E}$. Considering harmonic fields ($\frac{\partial}{\partial t} = j\omega$), the ratio of capacitive to resistive

currents is given by:

$$\frac{2\pi f \varepsilon_0 \varepsilon_r}{\sigma} \tag{3.16}$$

where ε_0 is the dielectric constant of free space, 8.85×10^{-12} C^2/Nm^2, and ε_r is the tissue relative dielectric constant. At a frequency of 10 kHz, the relative dielectric constant of many typical tissues is of the order of 10^5 and the conductivity is about 1 S/m, implying that the ratio of resistive to capacitive part of the tissue impedance is 0.0005. Thus, the small capacitive contribution to the tissue impedance can be neglected and the tissue treated as being purely resistive. This is equivalent to saying that any delays between the application of an electric field and the appearance of a charge distribution on the tissue surface are ignored. This approximation is weaker than the previous two, and may break down for higher frequencies and tissues with unusually small conductivities.

Applying the approximations mentioned above on equation (3.12) and (3.13), we are able to neglect the second derivative with time ($\partial^2/\partial t^2$)compared to that with space (∇^2). Thus (3.12) and (3.13) become:

$$\nabla^2 \vec{A} \cong \mu \vec{J} \tag{3.17}$$

$$\nabla^2 V \cong \frac{\rho}{\varepsilon} \tag{3.18}$$

Equation (3.18) is the Poisson equation. When there is no volume charge, i.e. $\rho = 0$, (3.18) reduces to Laplace's equation:

$$\nabla^2 V \cong 0 \tag{3.19}$$

This means that under quasi-static conditions, the potential V is found simply by solving the Laplace's equation (3.19).

Finally the tissue may be assumed to be a homogeneous, isotropic volume with a

simple geometry. This is clearly the least valid assumption, since all biological tissues are heterogeneous and some are anisotropic. The only justification for this assumption is that these calculations are only a relatively simple first step towards more accurate modeling. They also have an advantage in observing the behavior of various change of parameters.

3.1.3 Calculation of the induced fields

It is important to perform theoretical analysis to the induced electric fields in the biological tissue to understand the factors and parameters that affect magnetic neural stimulation. In this section, induced electric fields by a coil, carrying a time-varying current, are calculated, and the effect of coil shape and orientation with respect to the biological tissue is studied. The geometry of the problem is shown in Fig. 3.1 [34]

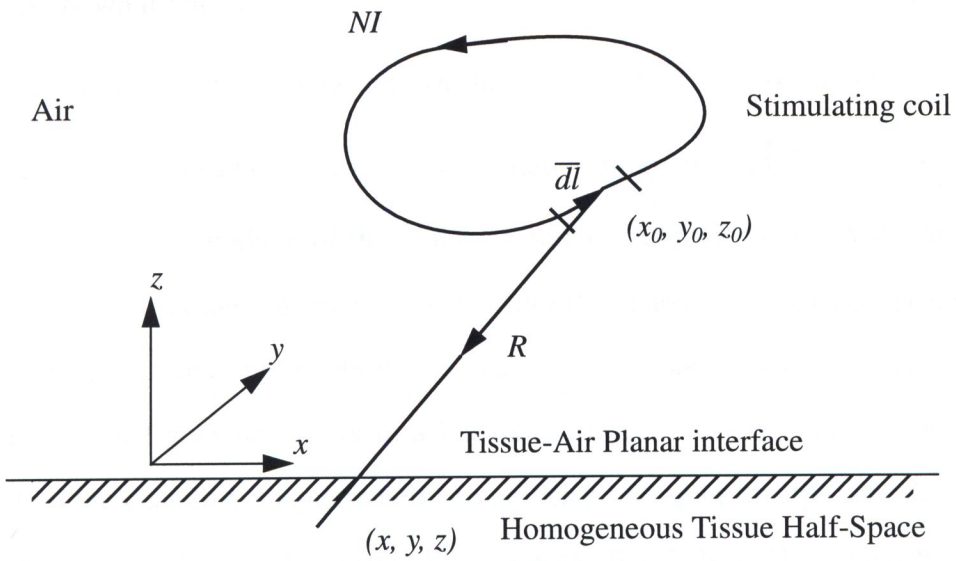

Figure 3.1 Schematic of induced E-field inside a semi-infinite conducting medium with an arbitrary coil configuration

The induced electric field is calculated from Faraday's law;

$$\nabla \times \vec{E} = -\frac{\partial}{\partial t}\vec{B} \tag{3.20}$$

where E is the electric field induced by the time-varying magnetic field $B(t)$ produced by the stimulating coil. As mentioned before, calculations are facilitated by expressing the magnetic flux density, B, as:

$$\vec{B} = \nabla \times \vec{A} \tag{3.21}$$

where A is the magnetic vector potential and is related to the coil current by the relation [10]:

$$\vec{A} = \oint_{coil} \frac{\mu_0 NI(t)}{4\pi r} \vec{dl} \tag{3.22}$$

where N is the number of coil turns, $I(t)$ is the coil current, dl is the infinitesimal coil length and r is the distance between the coil-element and the point where the field is calculated (as shown in Fig. 3.1).

As given by (3.11), the total electric field inside the tissue is due to two components: first, the component due to electromagnetic induction $-\partial\vec{A}/\partial t$ and second, the component due to the gradient of the scalar potential inside the tissue $-\nabla V$. Physically, this scalar potential is the potential resulting from the charge accumulation at the tissue boundary. To understand intuitively how a charge distribution arises, consider a circular coil in air oriented perpendicularly to a flat tissue surface [40]. The electric field lines produced by the changing magnetic field are circles pointing in the opposite direction to the current in the coil when the current is increasing (Fig. 3.2-a). These field lines cross the air-tissue interface. If this field is imposed on the tissue, then charge flows along the electric field lines until it reaches the tissue surface. Since the charge cannot flow into the air, which is an insulator, it accumulates on the tissue-air boundary; positive charge to the right of the coil, negative charge to the left. This surface charge distribution creates its own electric field (Fig. 3.2-b).

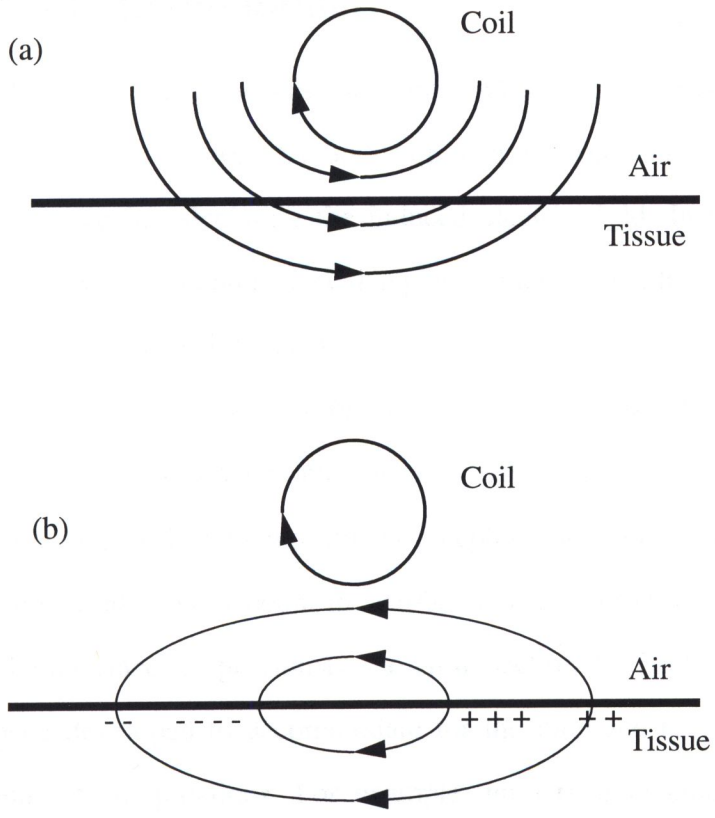

Figure 3.2 The electric field produced by a coil near tissue. This figure shows the qualitative behavior of the electric field lines, but is not intended to be quantitatively correct. (a) The electric field produced by the coil due to electromagnetic induction, E_A, and (b) the electric field produced by charge on the tissue surface, E_ϕ.

Charge accumulates until the component of the electric field perpendicular to the interface produced by this charge is equal and opposite to the normal component of the electric field produced by the time-varying magnetic field.

The first component is obtained by finding the magnetic vector potential $\vec{A}$ for a specific coil configuration in the region around the coil by using (3.22), while the second is obtained by solving the Laplace's equation (3.18) for a specific geometry and the associated boundary conditions.

3.2 Semi-infinite plane model

As indicated by (3.11), the air-tissue interface contributes to the induced electric field inside the tissue via the surface charge that builds up on it. Consequently, the shape of the interface is of importance in calculating the induced electric field. In this section, we consider a semi-infinite volume conductor with a planar interface while, subsequently, we consider cylindrical and spherical interfaces.

Despite the fact mentioned above, some investigations published earlier neglected the air-tissue interface, and the induced electric field was evaluated using analytical or semi-analytical techniques [41]. Although this is acceptable as a first approximation, an accurate analysis should take into account the surface charge on the interface unless the coil is parallel to the interface (as previously shown in section 3.1.3). Various numerical techniques have been developed to accommodate for the interface but they all require considerable amount of computations. For example, numerical techniques have been used to calculate the induced fields from a circular coil above a semi-infinite tissue space [28],[31]. The main limitation of these methods is the long computational time. Also, numerical solutions present inherent difficulties in gaining a physical insight into the dependance of the electric field and its spatial derivative on the coil geometry and neuron location.

Esselle and Stuchly have derived analytical expressions of the electric field and its spatial derivative in a semi-infinite tissue half-space due to an infinitesimal element of the current carrying coil [1]. The electric field and its spatial derivatives induced by an arbitrary shaped coil are then obtained by numerically combining the contributions from all elements forming the coil. The advantage of this technique is that the computation time is much less than the previous technique as the only numerical step is a one-dimensional integration. They have analyzed circular, square, and quadruple square coils. For

a single coil there are four equal (in magnitude) "hot-spots", two correspond to a hyper-polarization (positive peaks) and two for depolarization (negative peaks). Square coil has a stronger stimulus than the circular coil of comparable dimensions. Care has to be taken when stimulating nerves with such coils (single square or circular) in order to avoid slowing down (or even blocking) the propagation of the action potential due to the positive peaks. This effect is very much reduced when double square coils are used since the positive peak is 50% weaker than the negative peak. Those coils also have a stronger activating function than the single square or circular ones for the same pulse at the coil input. The quadruple square coil produces only one negative peak, just under the coil plane (which is useful when stimulating a shallow neurons) and therefore the volume of stimulation is more controllable. When stimulating deep neurons, quadruple square coils with an optimum spacing between individual squares are used to have only one peak at a given depth. They also show a stronger stimulus (a factor of 2) over the double-square coils.

All the calculations mentioned above showed that, regardless of the coil configuration considered, the electric field normal to the interface is always zero[1],[11],[42]. This means that the electric field inside the tissue is always parallel to the interface. It showed also that for long straight neurons the location of the stimulation depends only on coil configuration. For example, a neuron lying under a square coil is stimulated at a point corresponding to a corner of the coil. Fig. 3.3 shows the location of the stimulation of some coil configurations (half of the coil is only shown due to symmetry).

The advantage of the semi-infinite plane model is its simplicity, especially for coils oriented parallel to the interface. It also gives a good understanding of the factors affecting magnetic neuron stimulation without involved calculations. However, when stimulating peripheral neurons in the arm (e.g. ulnar nerve) or in the cortex, the semi-infinite plane model is no longer valid and a suitable geometry should be considered. For exam-

ple, for stimulating peripheral nerves in the arm or the leg a more suitable model is a cylinder, while for stimulating neurons in the cortex, it is a sphere. Those models will be discussed in some details in the following sections.

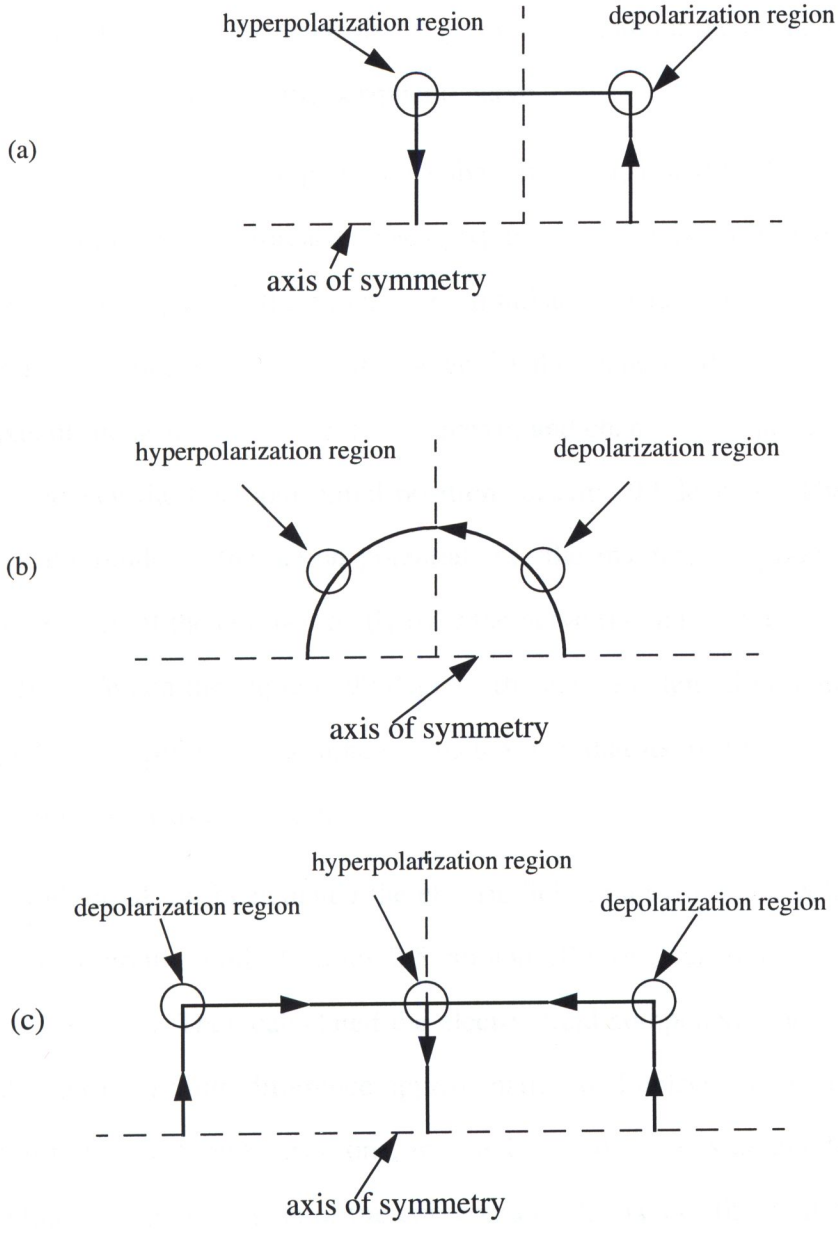

Figure 3.3 Location of the depolarization and hyperpolarization regions for: (a) square coil, (b) circular coil, and (c) a double-square coil. Due to symmetry, half of the coil is only shown.

3.3 Cylinder model

When stimulating peripheral neurons with coils that are of comparable size to the peripheral itself, the peripheral is better modeled as a cylindrical volume conductor. This model is of a great benefit in the sense that it gives an idea about the best coil configuration and orientation with respect to the peripheral nerve.

In an experimental report, Maccabee et al. [43] analyzed the problem of neuron stimulation in a human forearm. They positioned a circular coil of outer diameter of 9.2 cm on the volar part of the forearm to stimulate a distal median nerve. They measured the induced action potential in the nerve for the plane of the coil positioned parallel to the axis of the arm (i.e. parallel to the nerve) and changed this position in steps untill the angle between the final and initial positions became 90 degrees. They reported that the largest amplitude of the action potential (i.e. the maximum response of the neuron) is when the edge of the coil is directly over the nerve (i.e. tangential) and the coil is tilted to 45 degrees. When the angle is 90 degrees the action potential is reduced by 25%. However, when the coil was positioned in such a way that its axis is parallel to the nerve, the action potential was a minimum.

Roth et. al. [40] calculated the electric field in a cylindrical volume conductor produced by a circular coil of radius 2.5 cm and 10 turns, carrying a current changing at a rate of 100 A/μs. They calculated the electric field component due to the surface charge distribution by a finite difference approximation of Laplace's equation. They positioned the coil in two different ways: one, in which the coil axis is perpendicular to the axis of the cylinder while the plane of the coil contains the axis of the cylinder, and the other in which the coil axis is perpendicular to the axis of the cylinder while the plane of the coil is parallel to the axis of the cylinder (the coil is centered above the cylinder). They reported that, for the first coil orientation, the z-component of the electric field (z-axis is

taken as the axis of the cylinder), which is responsible for stimulating the peripheral neuron (median nerve), is largest (in absolute value) and negative at the arm surface and falls rapidly with distance away from the coil showing that the closer the neuron to the surface of the cylinder (toward the coil), the easier it is stimulated. For the second coil orientation, the z-component of the electric field was higher (in absolute value), an increase by a factor of 2 increase. This shows that the second coil orientation (coil plane is parallel to the tissue) is better to use for stimulating peripheral neurons.

D'Inzeo et al. [44] considered a homogeneous, nondispersive as well as a heterogeneous, dispersive model of the forearm. They digitized an anatomical picture of the forearm at the level of the third proximal by using a scanner. The stimulating coil, circular of radius 2.4 cm and 30 turns, was placed parallel to the surface of the arm in such a way that its edge was above the center of the arm (i.e. the coil not symmetrically placed). They used the finite difference technique to obtain the induced currents in the forearm. For the homogeneous, nondispersive case the points with highest current density are those at the skin and the current density decreases going deep into the tissue. They stated that in the homogeneous case the surface charge had a negligible effect. This is correct for the inside of the cylinder where there are no inhomogenuities. However, at the air-tissue interface, the effect of the surface charge is quite significant and should be taken into account. On the other hand, for the inhomogeneous, dispersive case the current density was lower than the homogeneous case and, therefore, the minimum coil current necessary to produce a neuron stimulation had to be increased.

In order to have better understanding of the parameters (for example coil dimensions, location and shape) affecting peripheral nerve stimulation in human arm, Esselle and Stuchly [45] derived an analytical solution of the induced electric fields in an infinitely long homogeneous cylindrical volume conductor during magnetic nerve stimula-

tion. They analyzed a perpendicular (vertical) circular coil and a tangential (horizontal) double-square coil. Their results were in a very good agreement with those reported by Roth et al. [40]. They showed that the axial field at the center of the cylinder is zero in agreement with what had been stated previously by Cohen and Cuffen [46]. Also, the double-circular coils showed a significant improvement (stronger and localized stimulus) over the vertically placed circular coil.

3.4 Sphere Model

When stimulating neurons in the human cortex a suitable model has to be used so that the induced electric fields are calculated with an acceptable accuracy. Since the anatomy of the human head is quite heterogeneous, an exact model will be too difficult to deal with.

Grandori and Ravazzanni [41] considered a homogeneous sphere model for magnetic stimulation of the motor cortex. They used circular, double-circular, and multicoil assembly for neuron excitation. Despite the fact that the surface charge on the air-tissue interface contributes to the induced field, as a first approximation, they neglected its effect and considered only the induced electric field by induction (coil contribution). Their results show that the induced electric field decays quickly going deep into the sphere. The volume of stimulation (the extend by which the induced electric field spreads into the sphere) increases also with depth. Better focality of the field is realized by the multicoil assembly than the double-circular and circular coils.

Roth et al. [13] analyzed a three concentric sphere model for magnetic stimulation of the cortex. The three layers represented the scalp, skull and cortex. The same model has been used before in modeling the EEG (it is the reverse process of the electric neuron stimulation, i.e. electrodes are used to measure the activity of a specific part in the brain) [47], [48]. Different conductivities were assigned to each layer [48]. In this analysis, the total induced electric field was the sum of two components: first component corre-

sponded to the coil, and the second was due to the surface charge. The second component of the electric field is obtained by solving Laplace's equation numerically (finite difference approximation). The three components of the electric field inside the model, the radial, r, the polar, θ, and the azimuthal, ϕ, produced by different coil configurations and orientations (circular and double-circular) were calculated. They concluded that, for all coil configurations and orientations, the radial component was much less than the other two components, approximately by two orders of magnitude. Also, among the coil configurations and orientations considered, a circular coil perpendicular to the sphere produced a more focused stimulus but a lower electric field than the tangential one. The double-circular coil produced a larger and more focused stimulation than other coil geometries used.

This model is a step forward as it accounts for the different layers of the head. However, the model does not account for the irregular shape of the head (especially the cortex) and assumes that it has a spherical shape. In reality, the cortex is divided into two adjacent parts. Two spheres corresponding to each side of the brain may be a better model. Another assumption is that the cortex is homogeneous and isotropic.

Because of the great advantage of the analytical solution in providing a better understanding of the parameters affecting a specific problem, Eaton [14] derived an analytical solution of a simple homogeneous sphere as the model of the head. The potential is expressed as an infinite sum of the spherical harmonic functions with suitable coefficients. The sum is then truncated after a sufficient number of terms to satisfy the convergence criteria. The excitation used is a double-circular coil (figure of eight) with different angles between its wings (each side of the coil is called a wing as the whole coil is sometimes called the butterfly coil). With the coil wings open, the field is stronger and more focal than it is when the wings are closed [14]. This analysis showed that the radial com-

ponent of the induced electric field is much smaller compared with the two other components (polar and azimuthal). This is in agreement with findings by Roth et al. [13].

The advantage of this model is that it can compute directly the total electric field inside the homogeneous spherical volume conductor for any practical excitation coil of any orientation. It can provide a high accuracy with a relatively short time on a PC. However, the model suffers from the disadvantages mentioned before.

Cuffin has suggested an eccentric spheres model of the head to account for the shift in both halves sides of the brain and to the variation in the thickness of the skull and scalp as well as the variation in the conductivity of the cortex [49]. Although the model concerns only the magnetoencephalography (MEG, the reverse process of magnetic brain stimulation), its results are partly useful for neuron stimulation, as the reciprocity theorem applies. The potential function in each region is expressed as an infinite sum of the associated Legendre polynomials with unknown coefficients. The coefficients are obtained by matching the boundary conditions at each interface. The variations in the thickness of the skull or the scalp and the inhomogeneity of the brain have a small effect on the spatial profile of the potential and the field. However, they have a significant effect on the amplitude. The variations in the skull and scalp thickness have much smaller effect on the field than the potential. Calculated differences in the maximum value of the potential are 10-30% as compared with the concentric spheres model. On the other hand, changes in the brain conductivity have a smaller effect on the field than the potential. Changes in the potential in this case are in the order of 10% [49].

3.5 Unresolved issues

Up until now, the neuron stimulation with the magnetic field has considered long, straight neurons. This leaves some important issues unresolved. For example, the activating function for long straight neurons is the spatial derivative of the electric field along the neuron [19],[20]. However, for finite-length nerves (terminated at one side), this is not true. Simplified models of such fibers show that the activating function is the electric field along the nerve and not its derivative [50]. This is in agreement with the experimental results obtained by Ueno et al. [51].

Another issue results from the fact that not all neurons are straight. More specifically, when modeling the magnetic stimulation for the human cortex, the shape of the neuron (which is no longer straight) will affect the location of the stimulation and consequently, the measured propagation time used in the diagnoses. It is also expected that different bend shapes will differently affect the location of the stimulation.

To summarize; two issues that need to be further considered are:

1- Bent neurons.

2- Terminal neurons.

In this theses, we only consider the first issue, namely the bent neurons.

Chapter 4

Magnetic stimulation of bent neurons in a semi-infinite plane

4.1 Problem formulation

The geometry of the problem is illustrated in Fig. 4.1. The nerve, indicated by line ABC, consists of two parts. A straight part, AB, and a bend, BC. The point B is the knee of the nerve, and the nerve is continuous at its knee. Beyond point C the nerve is straight in the z-direction (perpendicular to the interface). The nerve is assumed long compared to the dimensions of a stimulating coil so that the effects of the nerve terminations can be neglected. The nerve is located in a homogeneous tissue half-space and its straight part is parallel to the interface. The stimulating coil is in a plane parallel to the air-tissue interface and is centered above the nerve. In the real situation the nerve is stationary and the coil is positioned along the nerve to get the maximum stimulus. We will assume for the purpose of our analysis that the nerve is placed at different positions under the coil. Since the position is relative, we can evaluate the maximum stimulus (activating function). As shown in Fig. 4.1, there are two independent variables describing the location of the stimulation: The location of the nerve knee in x-direction, δ, and the horizontal distance in x-direction from the nerve knee, u. The solution for the maximum stimulus is obtained in two steps. First we consider the activating function along the nerve for a given δ. Next, we

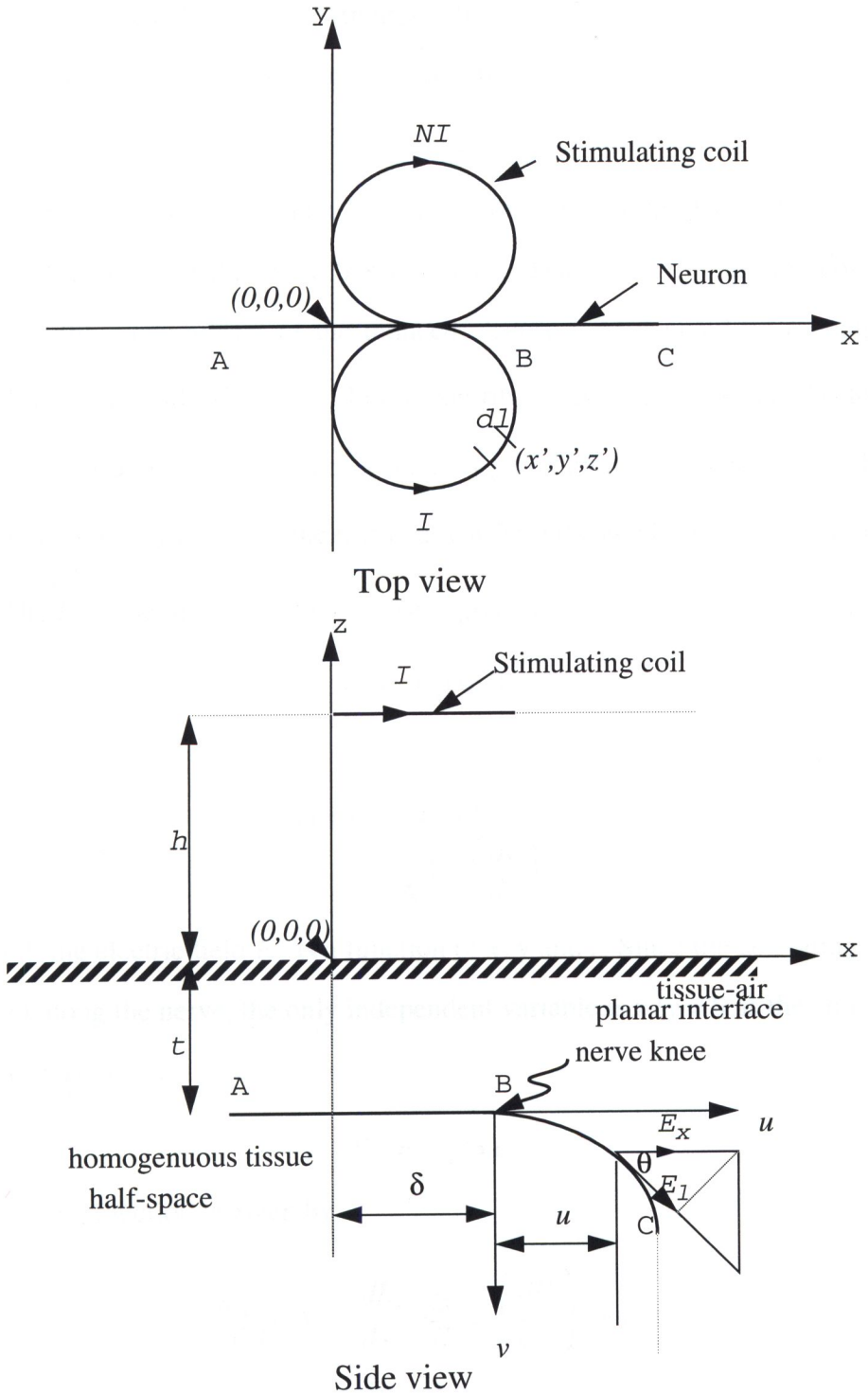

Figure 4.1 Geometry analyzed: the topfigure shows a double-circular coil (selected for illustration), and the bottom figure shows a straight nerve with a bend in a tissue half-space and the nerve position with respect to the coil. The coil has N turns, each carrying current I.

vary δ over a sufficiently large length under the coil.

The nerve shape is described by a general equation:

$$v = f(u) \tag{4.1}$$

Nerve stimulation is produced by the spatial derivative of the electric field along the nerve [5],[6]. Since the nerve lies in the x-z plane (Fig. 4.1) and the coil in the x-y plane, only the x-component of the induced electric field denoted by E_x contributes to nerve stimulation while E_y and E_z do not contribute, as E_y is perpendicular to the nerve and $E_z = 0$. For a curved nerve the stimulus is given by dE_l/dl where E_l is the induced electric field in the direction of the nerve, as earlier indicated by Basser and Roth [6].

The E_l in the direction of the nerve is given by

$$E_l = E_x \cos\theta \tag{4.2}$$

where

$$\cos\theta = \frac{1}{\sqrt{1 + \left(\frac{dv}{du}\right)^2}} \tag{4.3}$$

In general, the electric field E_x is a function of x, y and z. Since the activating function is computed along the nerve, the only independent variable is x ($y = 0$ as the coil is centered above the nerve), i.e.

$$E_x = E_x(x) \tag{4.4}$$

The activating function is given by

$$\frac{d}{dl}E_l(x) = \frac{dE_l}{dx} \cdot \frac{dx}{dl} = \left(\frac{dE_l}{dx}\right)\cos\theta \tag{4.5}$$

Since the variables x and u differ only by a constant, we can replace $\frac{d}{dx}$ by $\frac{d}{du}$.

Introducing this replacement to (4.5) we get

$$\frac{d}{dl}E_l(x) = \frac{dE_l}{du} \cdot \cos\theta \tag{4.6}$$

Substitution of (4.2) and (4.3) into (4.6) gives

$$\frac{dE_l}{dl} = \left(\frac{1}{\sqrt{1+\left(\frac{dv}{du}\right)^2}}\right)\frac{d}{dx}(E_x\cos\theta) = \left(\frac{1}{1+\left(\frac{dv}{du}\right)^2}\right)\frac{dE_x}{du} - \left(\frac{\left(\frac{dv}{du}\right)\left(\frac{d^2v}{du^2}\right)}{\left(1+\left(\frac{dv}{du}\right)^2\right)^2}\right)E_x \tag{4.7}$$

Equation (4.7) can be expressed as

$$\frac{dE_l}{dl} = T_1 \cdot \frac{dE_x}{du} + T_2 \cdot E_x \tag{4.8}$$

where

$$T_1 = \frac{1}{1+\left(\frac{dv}{du}\right)^2} \tag{4.9}$$

and

$$T_2 = -\frac{\left(\frac{dv}{du}\right)\left(\frac{d^2v}{du^2}\right)}{\left(1+\left(\frac{dv}{du}\right)^2\right)^2} \tag{4.10}$$

For straight nerves, the second term in equation (4.7) vanishes (as $\frac{dv}{du} = \frac{d}{du}f(u) = 0$) and the activating function reduces to the spatial derivative of the x-component of the electric field dE_x/du as previously stated by Basser et al. [5]. On the other hand, for curved nerves the second term does not vanish and the spatial derivative dE_x/du, as well as the electric field E_x contribute to the activating function dE_l/dl.

In general, the induced electric field during stimulation is produced by two

sources:(1) the current in the stimulating coil producing an electric field by electromagnetic induction, and (2) the induced surface charge on the air-tissue interface [13], [40]. Since we assume that the coils are positioned parallel to the air-tissue interface, there are no induced surface charges. The electric field at any point on the nerve is computed using the following relation

$$\vec{E} = -\frac{d\vec{A}}{dt} = -\frac{\mu_0 N (dI/dt)}{4\pi} \oint_{coil} \frac{1}{R} \vec{dl} \tag{4.11}$$

where

$$R = \sqrt{(x-x')^2 + (y-y')^2 + (z-z')^2} \tag{4.12}$$

$$x = u + \delta \tag{4.13}$$

$$y = 0 \tag{4.14}$$

$$z = t + v = t + f(u) \tag{4.15}$$

and dl is a coil length element, μ_0 is the permeability of free space ($4\pi x10^{-7}$ H/m), N is the number of coil turns, I is the current per turn, and R is the distance between the coil element located at (x', y', z') and the point on the nerve where the electric field is calculated.

4.1.1 Induced electric field by a double-circular coil

In this section, we calculate the induced electric field by a double-circular coil in a semi-infinite volume conductor with a planar interface. As equation (4.11) shows, the induced field is the time derivative of the magnetic vector potential $\vec{A}$. Therefore, our task is to calculate the magnetic vector potential $\vec{A}$ for the double-circular coil. We start by calculating the magnetic vector potential for a single circular coil. Then, the magnetic vector potential for the double-circular coil is obtained by superposition.

Fig. 4.2 shows the geometry of the coil. A circular coil of radius R lies in the plane

$z = 0$ of a cylindrical coordinate system (the radius of the wire is negligibly small). Due to the symmetry in the azimuthal direction, ϕ, the magnetic vector potential has only a ϕ-component. This component is given by [52]:

$$A_\phi = \frac{\mu_0}{4\pi}\oint\frac{I\cos\phi}{s}\vec{dl} \tag{4.16}$$

the distance s from the point $(R, \theta, 0)$ to the point $(r, 0, z)$ is given by:

$$s = \sqrt{z^2 + r^2 + R^2 - 2rR\cos\phi} \tag{4.17}$$

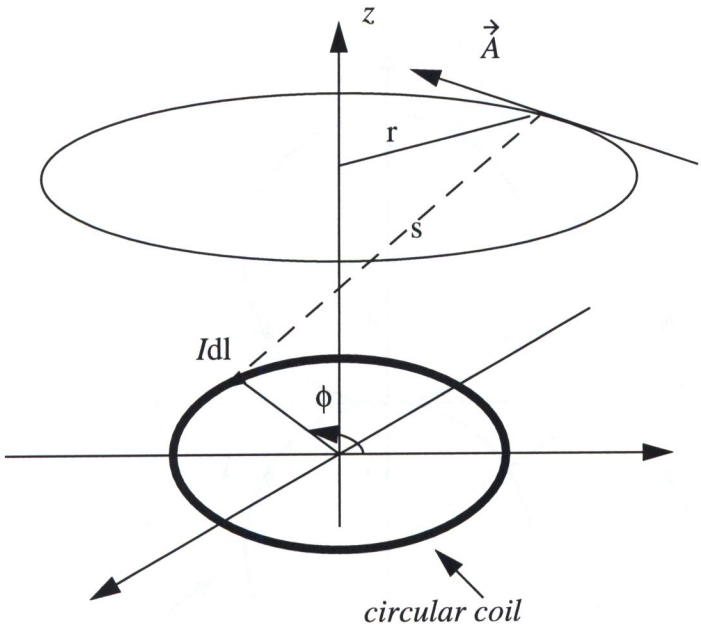

Figure 4.2 Geometry for calculating the magnetic vector potential for a circular coil

and the vector potential is obtained by integrating:

$$A_\phi = \frac{\mu_0 I}{4\pi} R \oint_0^{2\pi} \frac{\cos\varphi}{\sqrt{z^2 + r^2 + R^2 - 2rR\cos\phi}} d\phi \tag{4.18}$$

The integration is performed numerically using the Matlab mathematical package. As mentioned earlier, the total magnetic vector potential for a double-circular coil is obtained as the vector sum of individual contributions from each side of the coil. As Fig. 4.1 shows, we are interested only in the magnetic vector potential in the plane of the nerve, i.e. x-z plane. Fig. 4.3 shows a simplified configuration sufficient for our analysis.

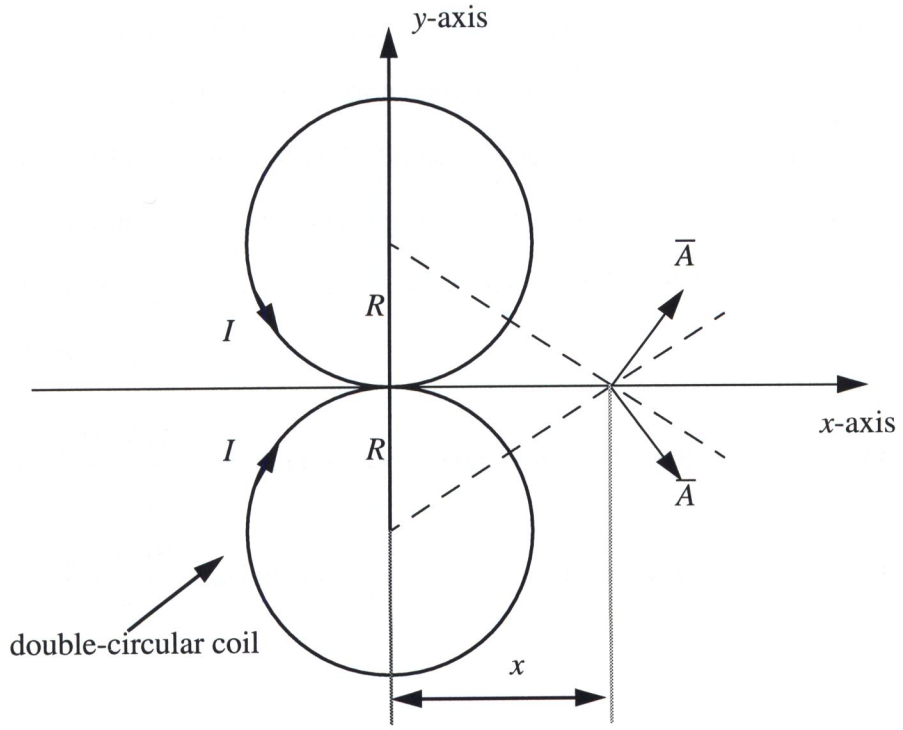

Figure 4.3 Magnetic vector potential for a double-circular coil in the plane of the neuron

The total magnetic vector potential is in the x-direction as the other component (in the y-direction) is cancelled. The total magnetic vector potential at any point in the x-z

plane is given by:

$$A_x(x,z) = 2A_\phi \frac{R}{\sqrt{x^2+R^2}} \tag{4.19}$$

where A_ϕ is given by (4.18). Finally, the induced electric field by the double-circular coil in the x-z plane is:

$$E_x = -\frac{\partial}{\partial t} A_x(x,z) \tag{4.20}$$

4.1.2 Induced electric field by a double-square coil

Esselle and Stuchly [53] derived an analytical formula to compute the induced electric field by a linear coil segment of length L carrying a current I. Using this formula, the induced electric field by any coil configuration composed of linear segments (in our case it is a double-square coil composed of eight linear segments) is directly obtained as the vector sum of all contributions of the linear segments. For a linear segment parallel to the x-y plane extending from (x_1, y_1, z_0) to (x_2, y_2, z_0), as shown in Fig. 4.4, the induced electric fields are given by [53]:

$$E_x = \frac{\mu_0 (\partial I/\partial t)}{4\pi} [\operatorname{asinh}(\cot\alpha_2) - \operatorname{asinh}(\cot\alpha_1)] \cos\theta \tag{4.21}$$

$$E_y = \frac{\mu_0 (\partial I/\partial t)}{4\pi} [\operatorname{asinh}(\cot\alpha_2) - \operatorname{asinh}(\cot\alpha_1)] \sin\theta \tag{4.22}$$

where

$$\alpha_1 = \operatorname{acos}\left[\frac{(x_1-x)(x_1-x_2) + (y_1-y)(y_1-y_2)}{R_1 L}\right] \tag{4.23}$$

$$\alpha_2 = \operatorname{acos}\left[\frac{(x_2-x)(x_1-x_2) + (y_2-y)(y_1-y_2)}{R_2 L}\right] \tag{4.24}$$

$$R_1 = \sqrt{(x-x_1)^2 + (y-y_1)^2 + (z-z_0)^2} \tag{4.25}$$

$$R_2 = \sqrt{(x-x_2)^2 + (y-y_2)^2 + (z-z_0)^2} \tag{4.26}$$

$$\theta = \operatorname{atan}\left(\frac{y_2 - y_1}{x_2 - x_1}\right) \tag{4.27}$$

The spatial derivatives of the electric field components are obtained by direct differentiation of equations (4.20) and (4.21).

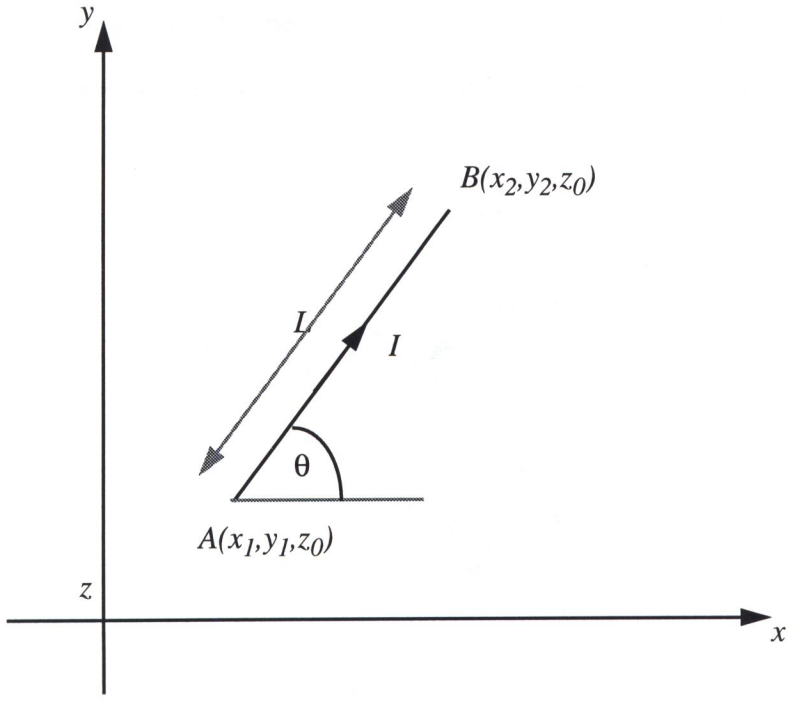

Figure 4.4 A linear coil segment of length L, parallel to the x-y plane and carrying a current I.

4.2 Results

Double square and double circular coil shapes were analyzed. Three nerve shapes were considered: cosh, parabolic and circular with different radii, as shown in Fig. 4.5 (Beyond point C in Fig. 4.1 the nerves are assumed perpendicular to the interface, this is not a critical assumption provided the nerves are not terminated). Stimulating coil is placed 1 cm above the air-tissue interface (i.e. h = 1cm). The straight part of the nerve is assumed to be 1cm below the interface (i.e. t = 1 cm). Coil dimensions are: 5cm x 5cm (a side) for the double-square coil and 5 cm diameter for the circular coil.The coil is placed in such a way that its longer dimension is perpendicular to the nerve (Fig. 4.1). The number of turns in each part of the coil and the time rate of change of the current I are N = 10 (total N = 20) and dI/dt = 100 A/μs.

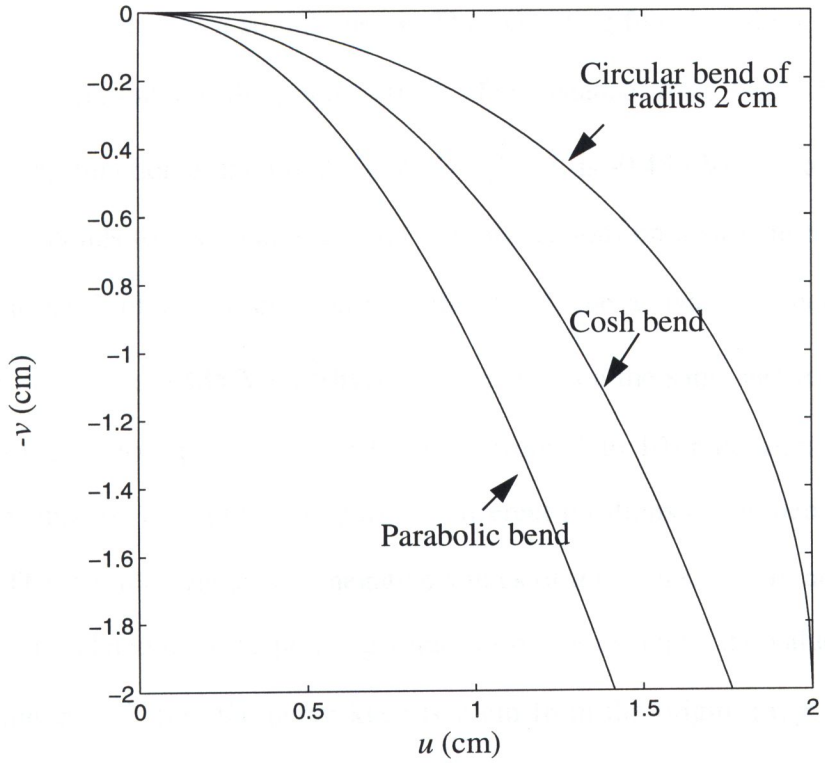

Figure 4.5 Nerve bends analyzed

The activating function is plotted in Fig. 4.6 as 3-D and as contours with two independent variables, u (the u-coordinate of the point on the bent part of the nerve with respect to the u-v axis) and δ, (the location of the knee under the coil). The contour showing the lowest value of the activating function corresponds to 10% above the absolute minimum, other contours are spaced by 20%.

Figs. 4.6 show the activating function dE_l/dl produced by the double-square coil along bends of the following shapes: cosh, parabolic and circular of radius 2cm. From the contour plots we can identify two sets of points. The points for $u = 0$ and δ from -5 to 10, and the points for $u > 0$ and δ from -5 to 10. The first set of points is represented in the contour plots by a vertical line $(0,\delta)$. However, in the physical problem the points $(u, \delta) = (0, \delta)$ represent a straight line at a depth t below the air-tissue interface. This line can be thought of as a straight nerve. The activating function along it is given by the values of the contours at the points $(0, \delta)$. For instance, from Fig. 4.6-*a*, the value of the activating function at the point $(u, \delta) = (0, 5)$ is -0.485 V/cm^2 (a minimum). This value corresponds to a stimulation point (depolarization) on a straight nerve lying in the tissue at a depth of $t = 1$ cm. On the other hand, the activating function at the point $(u, \delta) = (0, 0)$ is 0.485 V/cm^2(hyperpolarization) on the same nerve. The other set of points on the contour plots (i.e. $u > 0$ and δ from -5 to 10) represents the value of the activating function along the bent part for different positions of the bend with respect to the coil. The stimulus values for negative values of u (i.e. $u < 0$) are not shown as they can be easily related to corresponding values of δ. For example, the value of the stimulus at the point $\delta = 2$ (i.e. the nerve knee is 2 cm from the origin $(x, y, z) = (0, 0, 0)$) and $u = -1$, which corresponds to a point on the straight part of the nerve, is the stimulus value for $\delta = 1$ (i.e. the nerve knee is 1 cm from the origin (0,0,0) and $u = 0$ which

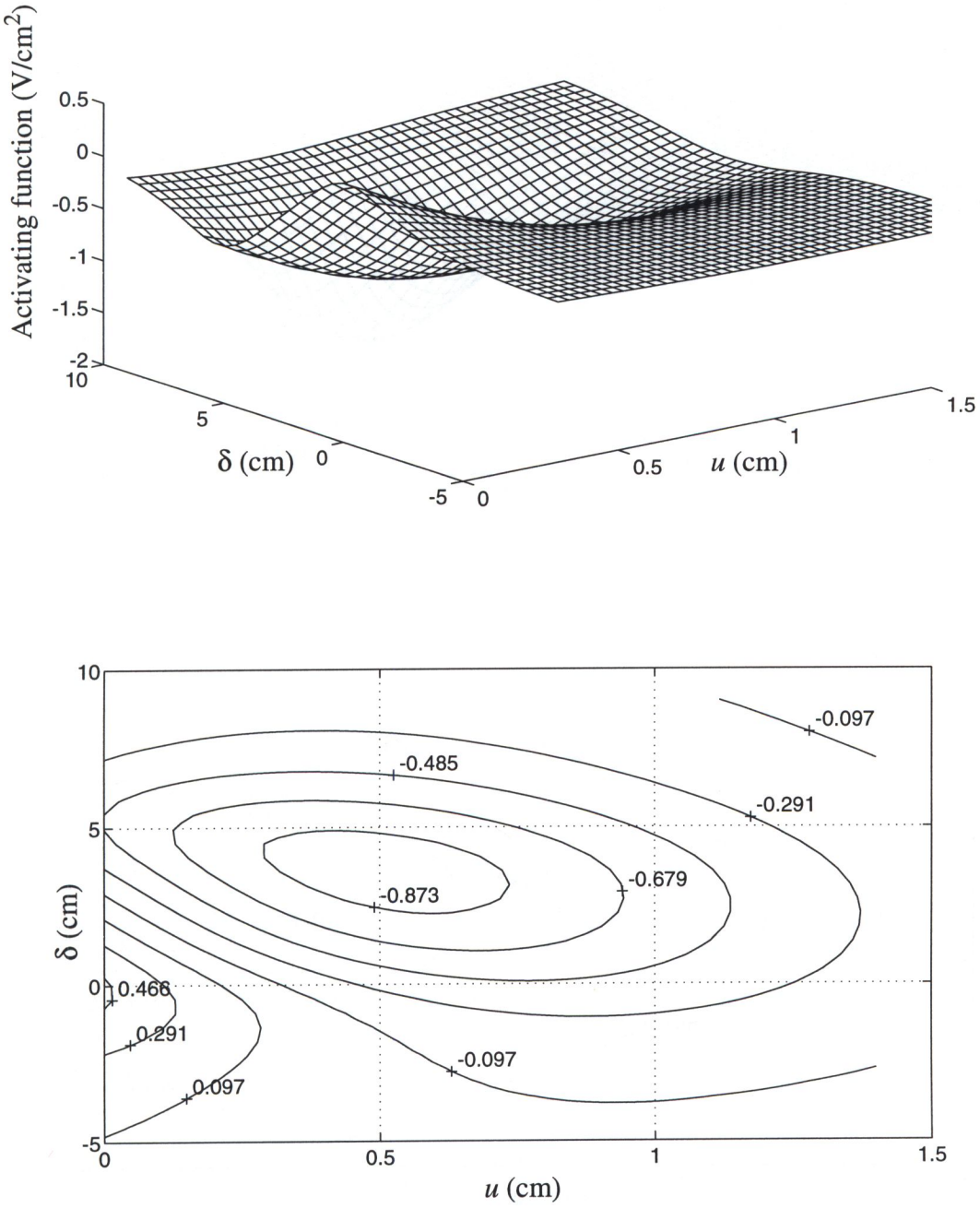

(a)

Figure 4.6-a 3-D and contour plots of dE_l/dl along a straight nerve with a bend. The stimulus (dE_l/dl) is produced by a 5x5 cm double-square coil parallel to the air-tissue interface. The 10-turn coil carries a current raising at 100 A/μs. The straight part of the nerve is 1 cm below the air-tissue interface. A cosh bend.

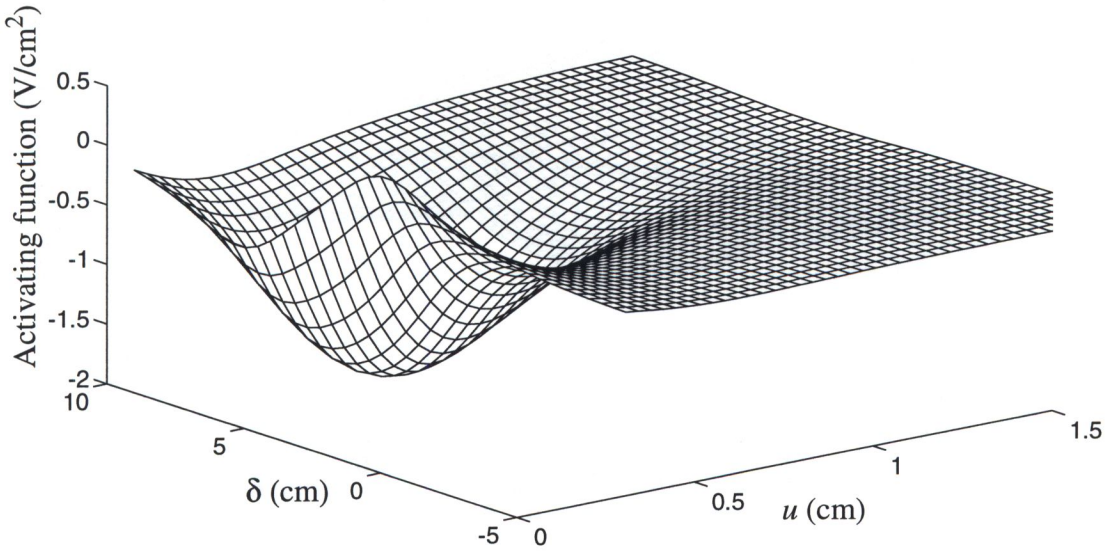

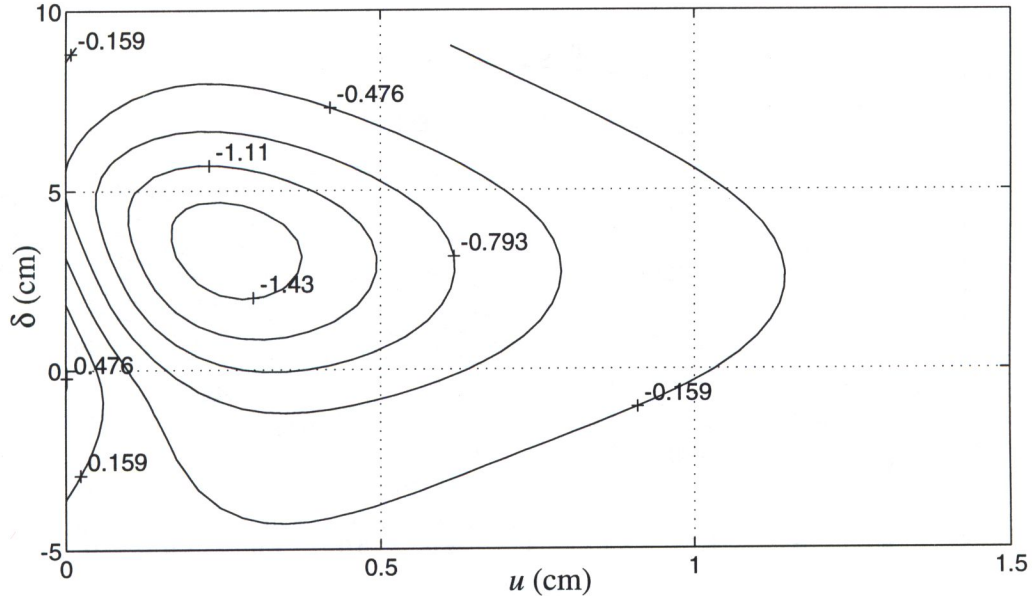

(b)

Figure 4.6-b 3-D and contour plots of dE_l/dl along a straight nerve with a bend. The stimulus (dE_l/dl) is produced by a 5x5 cm double-square coil parallel to the air-tissue interface. The 10-turn coil carries a current raising at 100 A/μs. The straight part of the nerve is 1 cm below the air-tissue interface. A parabolic bend.

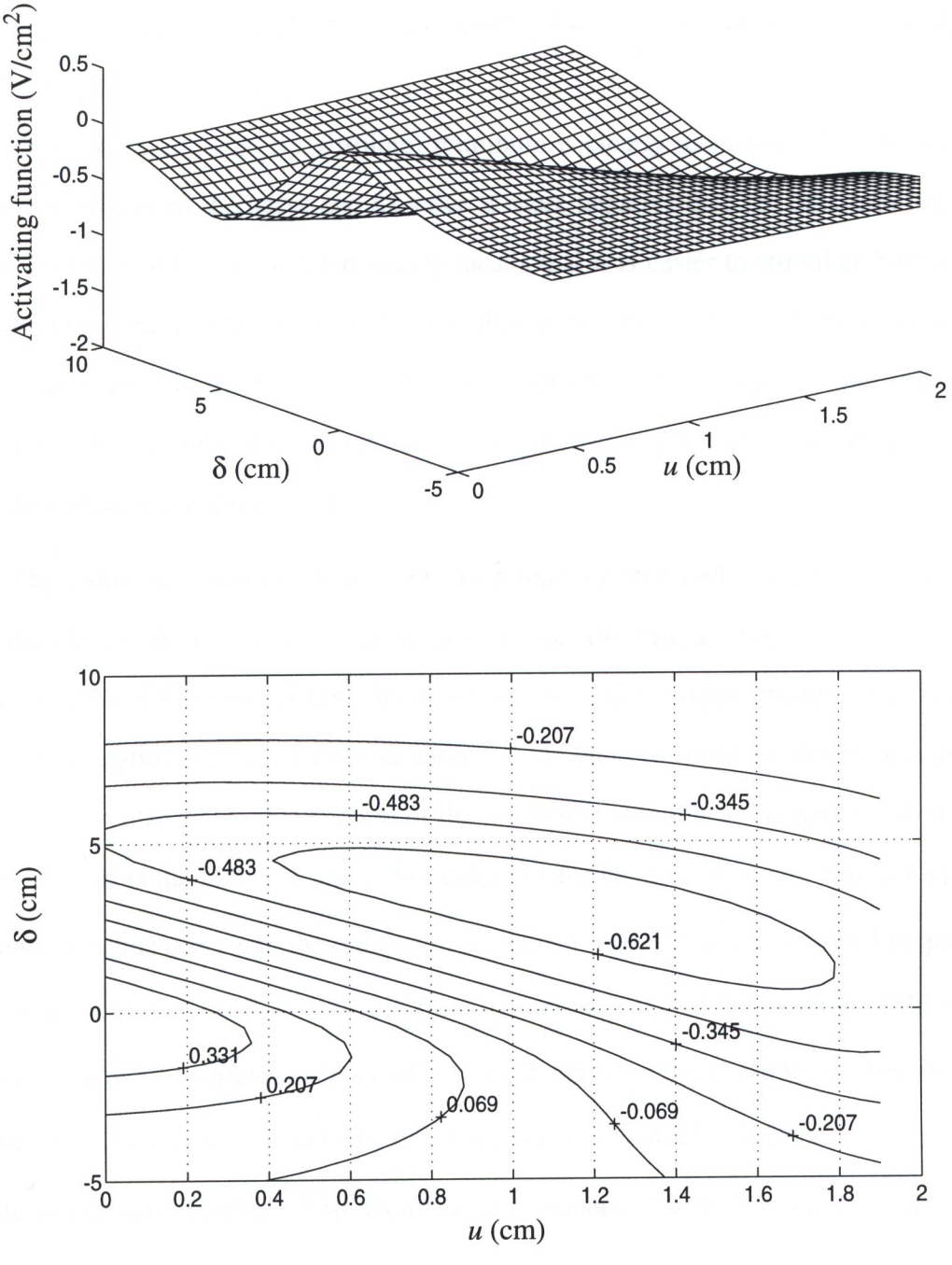

(c)

Figure 4.6-c 3-D and contour plots of dE_l/dl along a straight nerve with a bend. The stimulus (dE_l/dl) is produced by a 5x5 cm double-square coil parallel to the air-tissue interface. The 10-turn coil carries a current raising at 100 A/μs. The straight part of the nerve is 1 cm below the air-tissue interface. A circular bend of 2 cm radius.

is the end of the straight part for the nerve position $\delta = 1$ cm. The same argument holds for all other negative values of u.

In the plots, a global (or absolute) minimum is clearly identified. This minimum is on the curved part of the nerve and its value is more negative than the other minimum on the straight part of the nerve. That simply means that it is easier to stimulate bent nerves at their curved parts. This is due to the fact that at the curved part both the electric field and its derivative contribute to the activating function while only the derivative contributes in the straight part. This result of our analysis is in agreement with the previously published experimental results [4].

The value and location of this activating function (the global minimum) produced by a double-square as well as a double-circular coil for various shapes of the nerve are shown in Table 4.1. From this table it can be seen that, for a circular bend, the position of the maximum stimulus varies with the radius of the bend for both the double-square and the double circular coils. The location of the maximum stimulus at the nerve with respect to the coil axis is the sum of δ and u. For example, for the double square coil and a circular bend of radius $a = 1$ cm, the maximum stimulus (-1.61 V/cm^2) is obtained by placing the coil at a distance of $\delta = 1.78$ cm from the nerve knee and the location of the maximum will be at a horizontal distance of $u = 0.91$ cm from the nerve knee. However, for a larger bend radius $a = 3$ cm, the coil position is $\delta = 4.22$ cm from the nerve knee and the maximum stimulus (-0.56 V/cm^2) is at a distance of $u = 0.78$ cm from the nerve knee.

Table 4.1. The value and location of the maximum stimulus produced by a double-square and a double circular coils for different bend shapes.

Bend shape		Double-square			Double-circular		
		u (cm)	δ (cm)	$dE_l/dl\|_{max}$ $\left(V/cm^2\right)$	u (cm)	δ (cm)	$dE_l/dl\|_{max}$ $\left(V/cm^2\right)$
Cosh		0.49	3.70	-0.97	0.57	2.82	-1.33
Parabolic		0.26	3.39	-1.58	0.28	2.92	-1.71
Circular	a = 1cm	0.91	1.78	-1.61	0.74	2.19	-1.73
	a = 2cm	1.08	3.25	-0.69	0.92	2.19	-1.22
	a = 3cm	0.78	4.22	-0.56	1.08	2.19	-1.17

Another observation from Table 4.1 is that the stimulation threshold is the lowest for the greatest curvature of the bend. For instance, for the circular bends it is the lowest for the smallest radius analyzed (a = 1 cm). This result is in agreement with experimental data given by Maccabee et al [4], showing the lowest threshold for 90 degrees angle. It can also be seen from Table 1 that the double-circular coil produces a higher activating function than the double-square coil of similar dimensions. This is in contrast with the results obtained for straight nerves [1].

Comparing the contour plots we see that the nerve with a parabolic bend has the smallest volume of stimulation (which is proportional to the 10% contour width) while for the circular bend the 10% contour is elongated.

4.3 Discussion and conclusions

An analysis of stimulation with magnetic fields of bent neurons indicates that the stimulation occurs at the bent part of the nerve. This analysis considers long nerves whose terminations are sufficiently far away from the stimulating coil. The location and

magnitude of the activating function depend on the nerve shape and several parameters of the coil. Coil shapes analyzed include double-square and double-circular. The circular coils produce stronger stimuli, but square coils produce a more focused (smaller) volume of stimulation. Although the model analyzed is greatly simplified as compared with the actual anatomy and physiology of neural stimulation, it is believed to provide some useful information for clinical applications and a starting point for further analysis. The results of our analysis are in excellent qualitative agreement with experimental data reported by Maccabee et al [4].

Chapter 5

Magnetic stimulation of bent neurons in the human head

5.1 Introduction

In chapter 4, the parameters affecting the magnetic stimulation of bent neurons in a semi-infinite space were analyzed. It is also of importance to analyze bent neurons in the human head, as the analysis done in chapter 4 gives only an idea of how the different bend shapes affect different parameters in the neural stimulation and is of limited use in the clinical practice. Motor neurons usually originate from the control part of the brain (e.g. the part of the brain controlling the foot) and continue on the brain surface to the spinal cord and then to the peripheral muscles. In this chapter, we model the magnetic stimulation of the cortex for such neurons. In the model, we also take into account the inhomogenuity of the head. The model consists of a sphere representing the skull and scalp, and two smaller spheres of different conductivity inside the outer sphere, each represents a side of the brain.

5.2 Model of the human head

As shown in Fig. 5.1, the model consists of three spheres. The outer sphere of radius R_1 (cm) and conductivity of σ_1 (S/m) represents the scalp and skull. The two halves of the

brain are represented in this model by two spheres, each of radius R_2 (cm) and conductivity σ_2 (S/m). The two spheres are separated by a distance d (cm), and their centers is c (cm) above the x-y plane . The x-z plane passes through the centres of the three spheres.

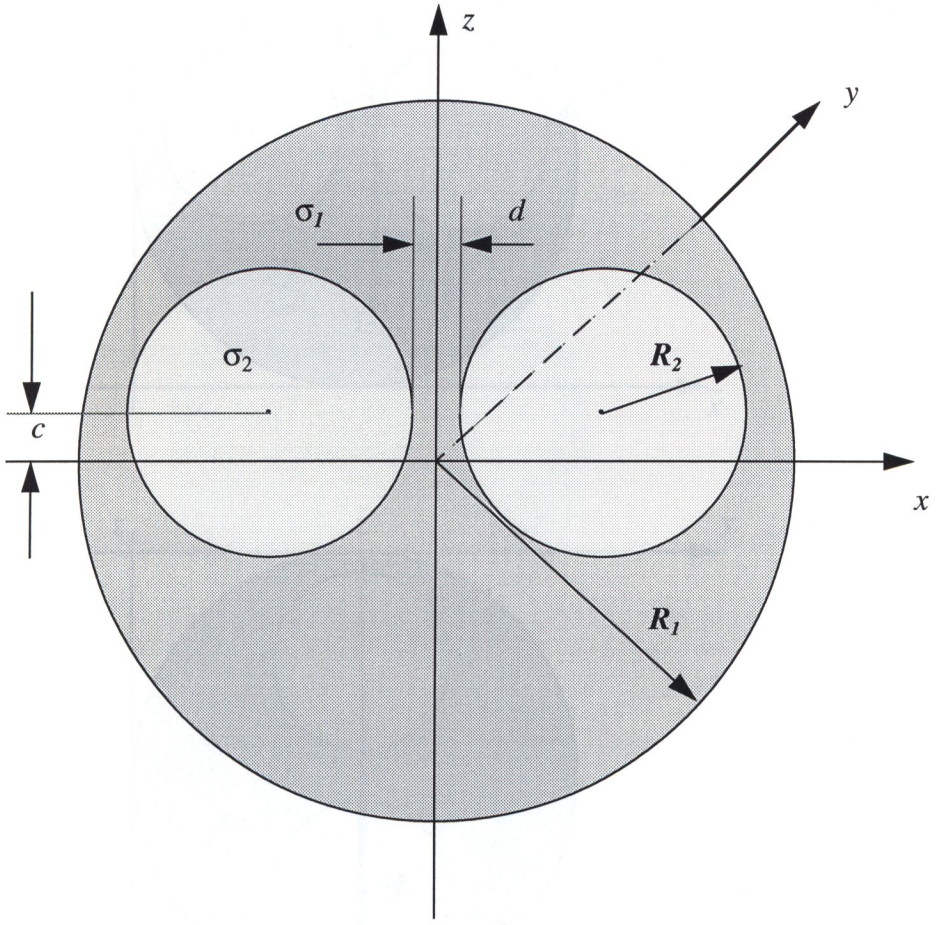

Figure 5.1 Geometry of the model for the human head. A sphere of radius R_1 represents the scalp and skull, and two spheres of radius R_2 represent the two halves of the brain.

Coil and neuron positioning are shown in Fig. 5.2. Fig. 5.2-a shows a cross section in the plane $\bar{x}$-$\bar{z}$ parallel to the x-z plane. The cross section passes through the centers of the three spheres. Fig. 5.2-b is a top view showing the nerve position.

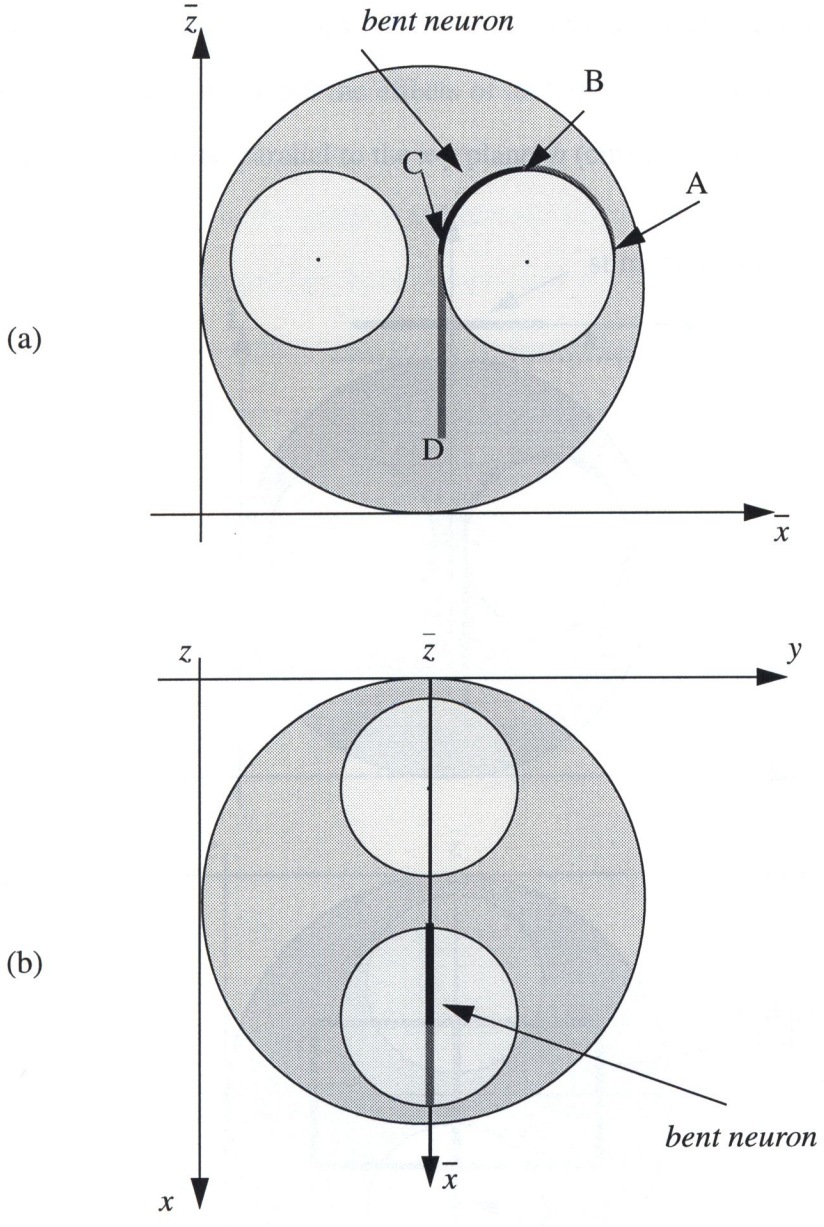

Figure 5.2 The geometry of the problem and the neuron position. (a) A cross section parallel to the x-z plane. (b) A top view (outer shell partly transparent)

The neuron originates from the surface of the brain (point A), continues on the surface of the brain passing through points B and C with a circular shape, and then goes down in the spinal cord (point D Fig. 5.2). The neuron is assumed to be in the plane parallel to the x-z plane ($\bar{x}$-$\bar{z}$ plane). The nerve is assumed long compared to the dimensions of the stimulating coil so that the effects of its terminations can be neglected. The stimulating coil is in a plane parallel to the x-y plane, h (cm) above the outer sphere (Fig. 5.3).

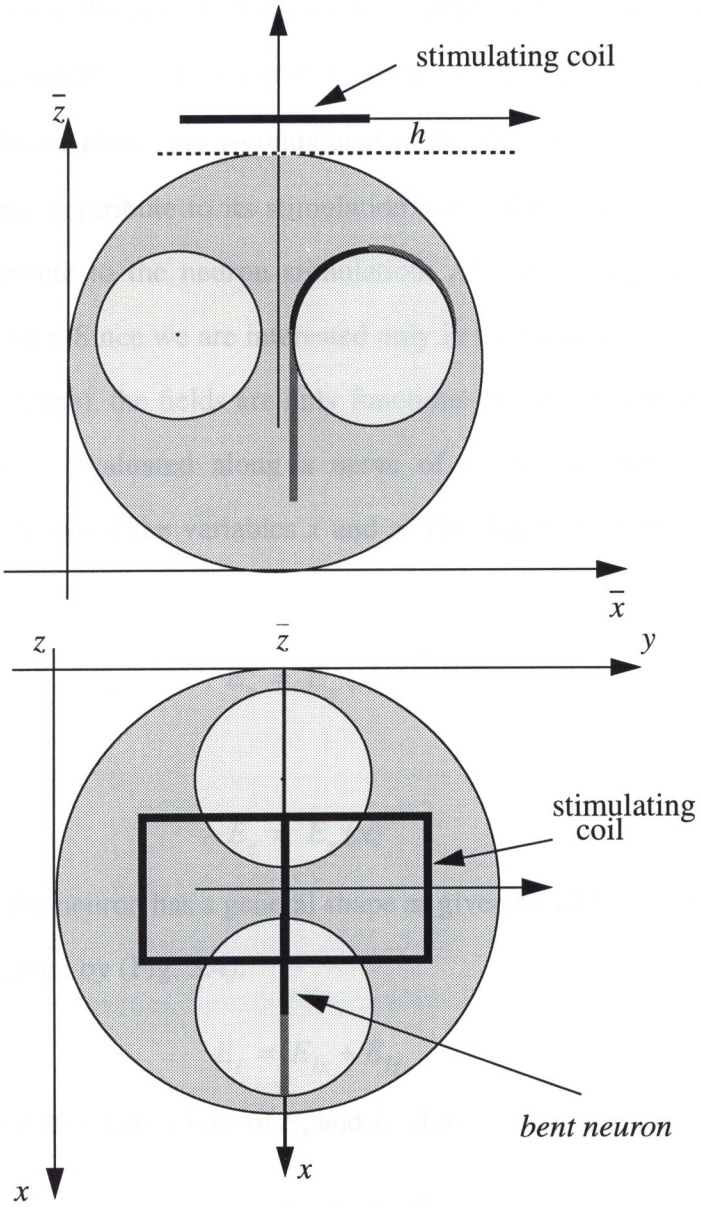

Figure 5.3 Relative coil position.

The coil is centered above the nerve (in the y-direction) with its longer dimension perpendicular to the plane of the nerve (in Fig. 5.3, a double-square coil is used for illustration). This orientation of the coil is selected for the optimal stimulation as reviewed in chapter 3 and analyzed in chapter 4. The activating function is the spatial derivative of the electric field along the nerve [5],[6]. The maximum stimulus is obtained by considering the activating function along the nerve for a certain coil position. Then the coil position is varied in steps in the positive x-direction. In general, the total induced electric field inside the spherical model has three components E_x, E_y, and E_z. Since the nerve lies in a plane parallel to the x-z plane, the y-component of the electric field, E_y, is normal to the neuron and does not contribute to its stimulation. Only the x- and z-components of the electric field contribute to the neuron stimulation. All field components are generally functions of x, y, and z. Since we are interested only in the fields in the plane of the nerve (parallel to the x-z plane), the fields are only functions of x and z. On the other hand, the activating function is evaluated along a nerve of a specific shape (circular) which imposes a relation between the variables x and z. This leaves x as the only independent variable. We have:

$$E_x = E_x(x) \tag{5.1}$$

and

$$E_z = E_z(x) \tag{5.2}$$

Let us assume that the neuron has a general shape as given by (4.1). The total electric field along the nerve is given by (Fig. 5.4):

$$E_l = E_{lx} + E_{lz} \tag{5.3}$$

where E_{lx} and E_{lz} are the components of E_x and E_z along the nerve, respectively, given as:

$$E_{lx} = E_x(x)\cos\theta \tag{5.4}$$

$$E_{lz} = E_z(x)\sin\theta \tag{5.5}$$

where

$$\cos\theta = \frac{1}{\sqrt{1+\left(\frac{dv}{du}\right)^2}} \tag{5.6}$$

$$\sin\theta = \frac{\left(\frac{dv}{du}\right)}{\sqrt{1+\left(\frac{dv}{du}\right)^2}} \tag{5.7}$$

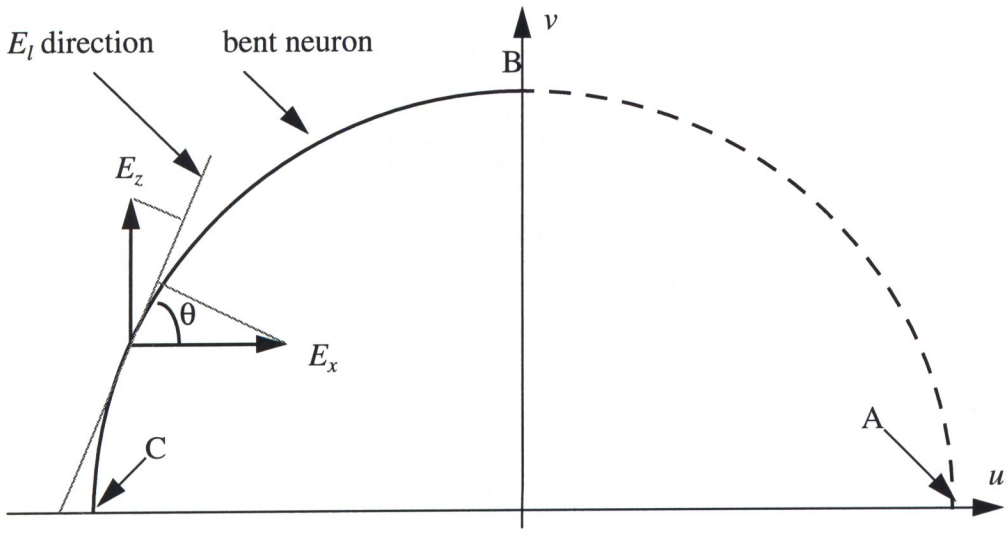

Figure 5.4 Bent neuron and field components contributing to its stimulation

The activating function is the spatial derivative of the electric field along the neuron. As shown in Fig. 5.4, the activating function is given by:

$$\frac{d}{dl}E_l(x) = \frac{dE_l}{dx}\cdot\frac{dx}{dl} = \left(\frac{dE_l}{dx}\right)\cos\theta \tag{5.8}$$

by substitution of (5.4) and (5.5) into (5.3), then substituting the result into (5.8), and

replacing the *d/dx* by *d/du* (since the variables x and u differ only by a constant), the activating function is expressed as:

$$\begin{aligned}\frac{d}{dl}E_l(x) &= \left[\frac{d}{du}(E_{lx}+E_{lz})\right]\cos\theta \\ &= \left[\frac{d}{du}[E_x(u)\cos\theta + E_z(u)\sin\theta]\right]\cos\theta \\ &= T_1\cdot\frac{dE_x}{du} + T_2\cdot E_x + T_3\cdot\frac{dE_z}{du} + T_4\cdot E_z\end{aligned} \tag{5.9}$$

where

$$T_1 = \frac{1}{1+\left(\frac{dv}{du}\right)^2} \tag{5.10}$$

$$T_2 = -\frac{\left(\frac{dv}{du}\right)\left(\frac{d^2v}{du^2}\right)}{\left(1+\left(\frac{dv}{du}\right)^2\right)^2} \tag{5.11}$$

$$T_3 = \frac{\left(\frac{dv}{du}\right)}{1+\left(\frac{dv}{du}\right)^2} \tag{5.12}$$

$$T_4 = \frac{\left(\frac{d^2v}{du^2}\right)}{\left(1+\left(\frac{dv}{du}\right)^2\right)^2} \tag{5.13}$$

Equation (5.9) shows that both the x- and z-components of the electric field and their derivatives contribute to the activating function of the bent neuron.

5.3 Method of solution

5.3.1 Impedance method

In chapter 4, the calculation of the activating function in a semi-infinite space was straight forward, as there was no surface charge distribution (the coil is parallel to the air-tissue interface) and the induced electric field was only due to the induction. However, in the problem we consider in this chapter, the air-tissue interface is spherical and the coil geometry is such that it produces a surface charge on the interface. As mentioned earlier, the induced field can be obtained by solving the Laplace's equation with the boundary conditions for the geometry under consideration. This can be done either analytically by expanding the potential function in terms of the spherical harmonic functions, or numerically, by using for instance the finite difference method. In either way, we also need to obtain the induced electric field by induction in a separate step [13],[14]. Finally, the activating function is obtained by summing its individual components.

Several existing numerical techniques, e.g., finite difference, finite element and TLM, have the advantage of obtaining the total induced field in one solution step by solving Maxwell 's equations under the existing excitation conditions.

The finite difference (FD) technique is widely used in computing the potential distribution in biological tissues [40]. For quasi-static problems the FD method can be conveniently used with the circuit representation rather than the field representation. Both the admittance [44] and the impedance formulation [54], [55] can be used. In our analysis, we are going to use the impedance method. The formulation of this method is quite similar to that of the admittance method.

To be able to use the impedance method to obtain the induced currents in the biological tissues, quasi-static conditions are assumed. This is equivalent to saying that the magnetic field produced by the excitation is not perturbed by the secondary magnetic field produced by the induced current. This condition is satisfied for the frequencies [56]

$$f \ll \frac{1}{\mu_0 \sigma L^2} \tag{5.14}$$

where σ is the conductivity and L is the largest dimention of the geometry analyzed.

Another simplifying assumption results from the electrical properties of biological tissues at frequencies of concern in this analysis, namely:

$$\sigma \gg 2\pi f \varepsilon' \tag{5.15}$$

where ε' is the dielectric constant ($\varepsilon' = \varepsilon_r' \varepsilon_0$). This assumption reduces the impedance network to the resistance network [54].

In the impedance method, the biological body is divided into parallelepiped volume cells. Each volume cell, as shown in Fig. 5.5-a [55], is represented by three resistances (Fig. 5.5-b). In the case of cubes and isotropic electrical properties of the biological tissue, the resistances in all directions are the same and equal to [54]

$$R^{i,j,k} = \frac{1}{\sigma^{i,j,k} \Delta} \tag{5.16}$$

where (i, j, k) denotes the computational node index, $\sigma_{i,j,k}$ is the conductivity of that volume and $\Delta = \Delta x = \Delta y = \Delta z$ is the side dimention of the cube (the grid length).

Fig. 5.5-c shows an arrangement of resistances of adjacent volumes (computational cells). Applying Kirchhoff 's voltage law for the loop in the *x-y* plane we have:

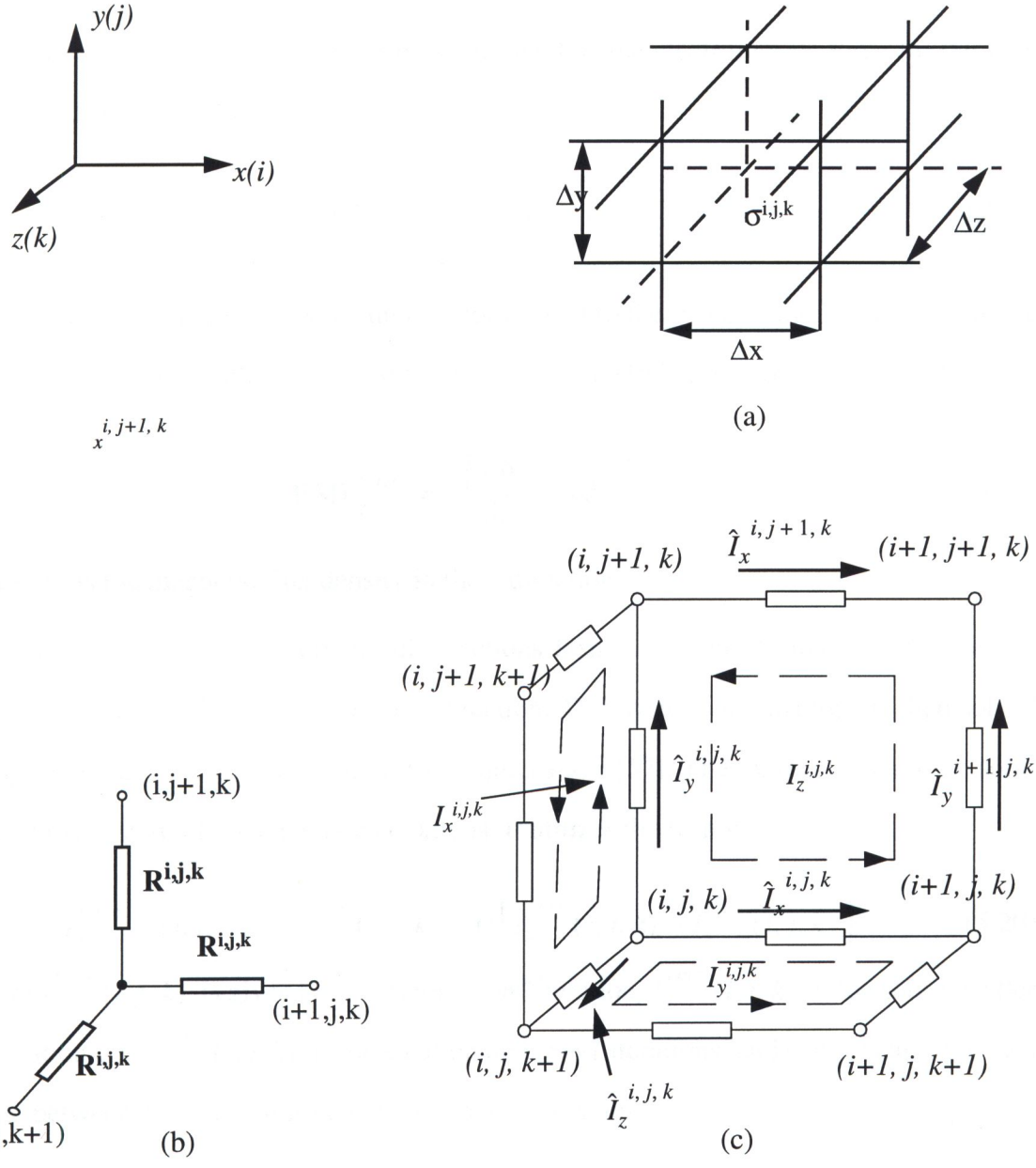

Figure 5.5 The designation of the variables in the impedance network method: (a) a cubical volume representing a part of the biological cell, which constitutes a computational cell; (b) three equivalent resistances connected to node *(i, j, k)* representing the volume in (a), and (c) line and loop currents associated with node *(i, j, k)*.

$$(\hat{I}_x R)^{i,j,k} + (\hat{I}_y R)^{i+1,j,k} - (\hat{I}_x R)^{i,j+1,k} - (\hat{I}_y R)^{i,j,k} = \mathrm{EMF}_z^{i,j,k} \tag{5.17}$$

where $\hat{I}_x$ and $\hat{I}_y$ are the branch currents, and EMF is the electromotive force for the loop given by Faraday's law as:

$$\mathrm{EMF}_z = -\left(\frac{\partial}{\partial t}\int_A \left(\vec{B}\cdot\vec{n}\right)ds\right) \tag{5.18}$$

where A is the loop area, $\vec{n}$ is the unit vector normal to the plane of the loop. For a square loop sitting in the x-y plane with a side length Δ, the EMF is given by:

$$\mathrm{EMF}_z^{i,j,k} = -\left(\frac{\partial B_z^{i,j,k}}{\partial t}\cdot\Delta^2\right) \tag{5.19}$$

where B_z is the magnetic flux density in the z-direction.

Loop equations for loops in all directions form a system of equations of size N^3, where N is the number of cells in each direction. This system of equations is then solved using the successive over-relaxation technique (SOR) [57]. The SOR is an iterative solution of the system of the algebraic equations. It utilizes the formula:

$$I_x^{(m+1)}(i,j,k) = I_x^{(m)}(i,j,k) + \alpha\left[\hat{I}_x^{(m)}(i,j,k) - I_x^{(m)}(i,j,k)\right] \tag{5.20}$$

where $\hat{I}_x^{(m)}(i,j,k)$ is given by (5.17) for the m^{th} iteration, $I_x^{(m)}(i,j,k)$ is the solution after m iterations, $I_x^{(m+1)}(i,j,k)$ is the solution after $m+1$ iterations, and α is a factor having a value between 1 and 2 and is called the *relaxation factor*.

5.3.2 Procedures of the numerical solution

In this section we show the general procedure for obtaining the induced fields using the impedance method. The procedure is as follows:

1- Include the geometry of the problem in a parallelepiped structure such that it contains all the geometry inside it. In the case of a spherical volume, a cube is a good choice as shown in Fig. 5.6-a.

2- Discretize the volume into small cells, parallelepiped or cubical, depending on the geometry, and assign an index to each node as well as a resistance (or in general an impedance) to each branch in the network (Fig. 5.6-b and c). Cell indices and the corresponding resistance values are stored in a file. The total number of cells in the volume, and consequently the cell size, is limited by the available computer facilities and by the computation time. This imposes a limit on the accuracy and maximum resolution. One million cells is a typical number for a medium size computer.

3- Compute the magnetic field of the coil (by integrating the magnetic field produced by an infinitisimal element over the coil geometry) at the discretized space occupied by the cubical volume and store the three components (x, y and z) of the magnetic field in a file.

4- Write down a recursive relation of the loop currents. Zero current values are always forced in the regions outside the volume (air regions).

5- Discretize the excitation in the volume under consideration.

6- Solve the system of equations using the iterative technique mentioned above. This way all loop currents are obtained, and from them the branch currents are calculated.

7- Finally, obtain the electric field by multiplying the conductivity associated with each cell by the corresponding current density. The latter is calculated by dividing the branch current by the loop area normal to it.

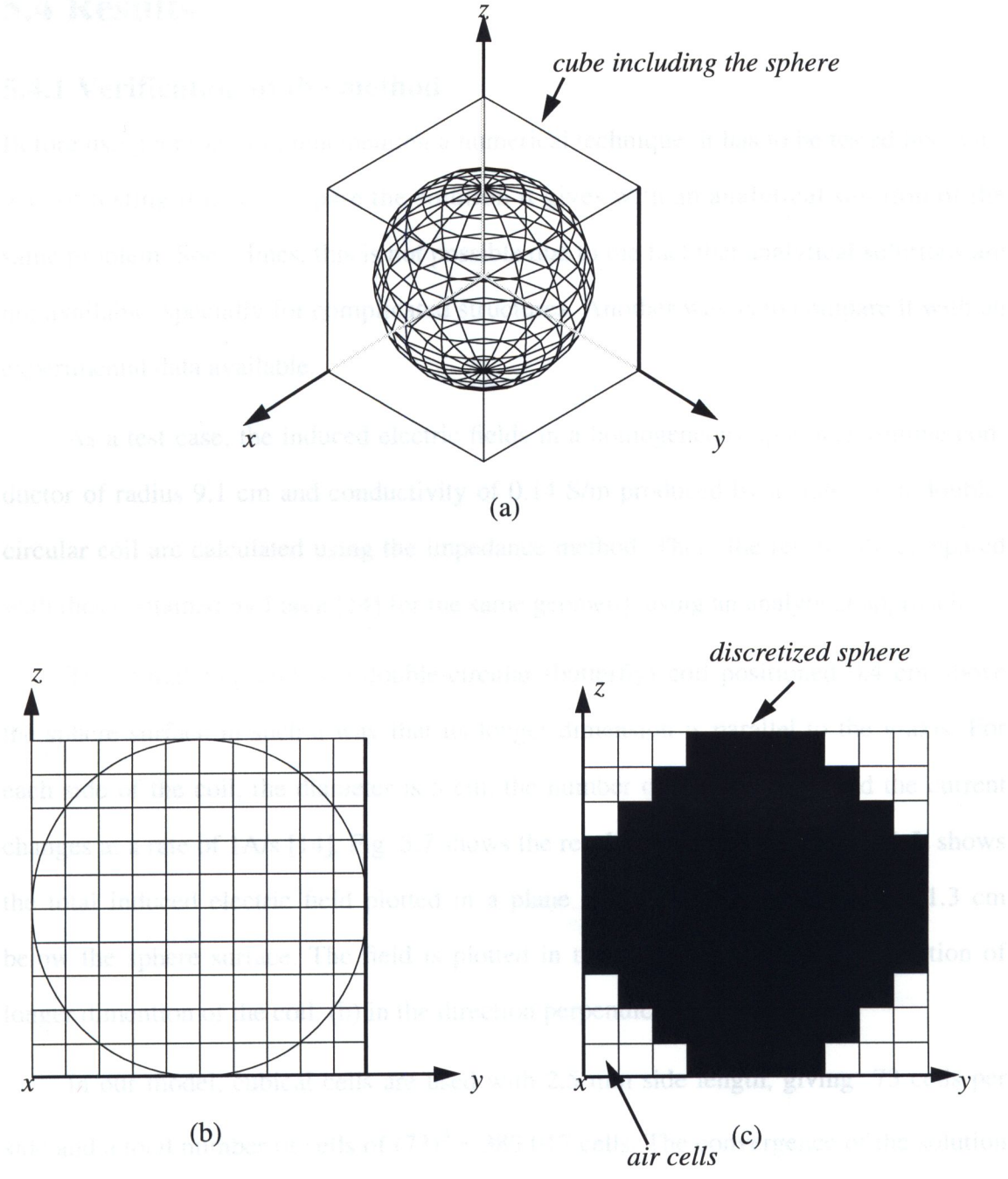

Figure 5.6 Steps of numerical solution. (a) The geometry included in a cubical. (b) Front view of the discretized volume. (c) The spherical volume after discretization.

5.4 Results

5.4.1 Verification of the method

Before using a program implementing a numerical technique, it has to be tested first. One way of testing it is to compare the solution it gives with an analytical solution of the same problem. Sometimes, this is not possible due to the fact that analytical solutions are not available, specially for complicated structures. Another way is to compare it with an experimental data available.

As a test case, the induced electric fields in a homogeneous spherical volume conductor of radius 9.1 cm and conductivity of 0.14 S/m produced by a single turn double-circular coil are calculated using the impedance method. Then, the results are compared with those obtained by Eaton [14] for the same geometry using an analytical approach.

The stimulating coil is a double-circular (butterfly) coil positioned 0.4 cm above the sphere surface in such a way that its longer dimension is parallel to the y-axis. For each side of the coil, the diameter is 5 cm, the number of turns is one , and the current changes at a rate of 1A/s [14]. Fig. 5.7 shows the results obtained by Eaton [14]. It shows the total induced electric field plotted in a plane parallel to the *x-y* plane and 1.3 cm below the sphere surface. The field is plotted in two directions: (a) in the direction of longer dimention of the coil. (b) in the direction perpendicular to that of (a).

In our model, cubical cells are used with 2.5 mm side length, giving 73 cells per side and a total number of cells of $(73)^3 = 389{,}017$ cells. The convergence of the solution is checked with the parameter, ζ, the summation of the magnitude of the electric field over all nodes. The iteration process is stopped when the relative error in ζ for two successive iterations is 5×10^{-4}. The solution is obtained after a number of iterations of 668 with an overall run time of about 30 minutes, on a workstation HP 9000 / 735.

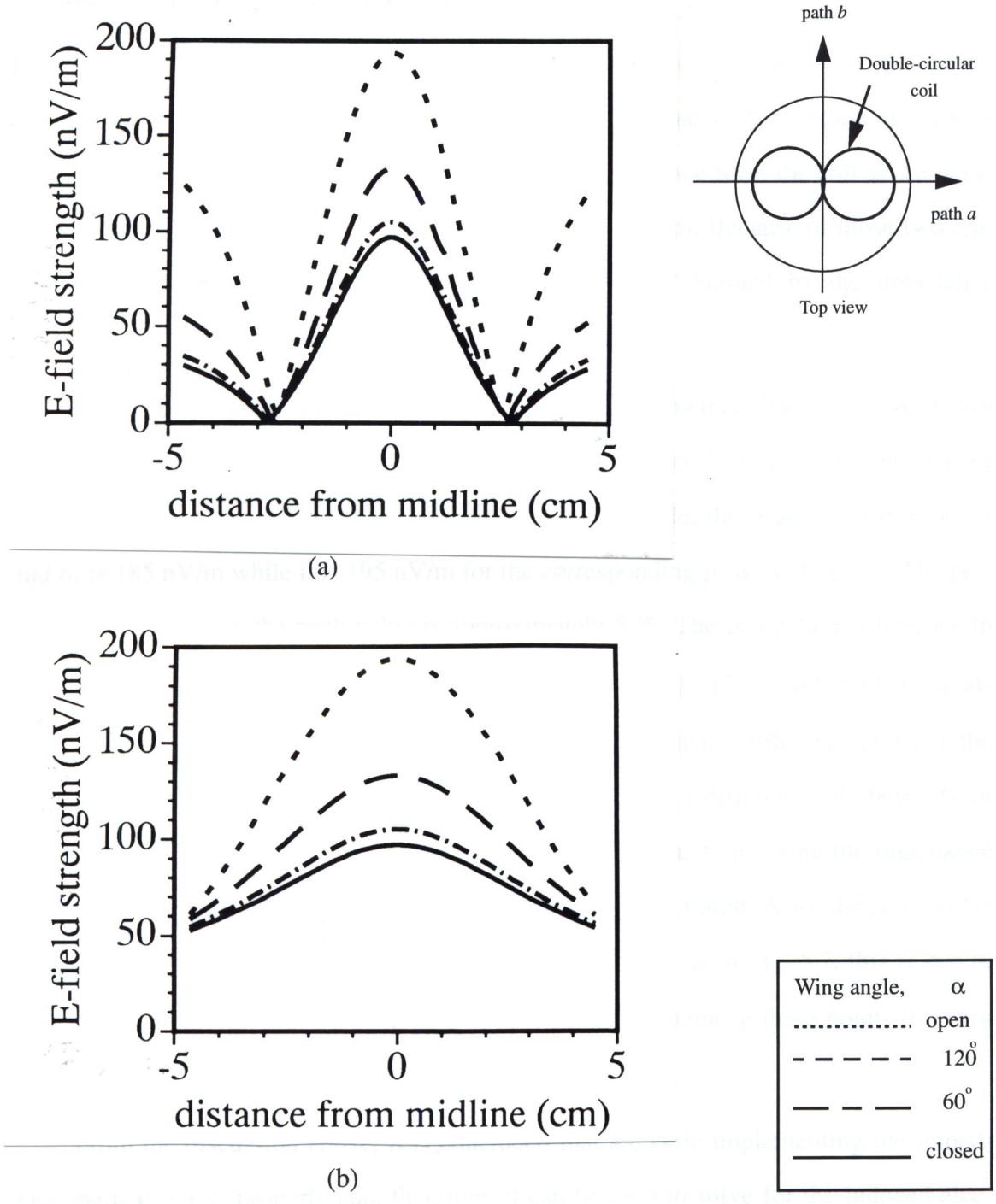

Figure 5.7 Results obtained by Eaton [14]: the magnitude of the electric field produced by butterfly coils having various "wing" angles excited with a current ramp of 1 A/s. (a) The field strength along path a in a plane 1.3 cm below the sphere surface. (b) The field strength along path b in a plane 1.3 cm below the sphere surface.

Due to the discretization selected (selected to be suitable for computations of the head model), it is only possible to position the coil 0.5 cm above the sphere surface (compared to 0.4 cm used by Eaton) and to plot the field in a plane 1.25 cm below the sphere surface (compared to 1.3 cm used by Eaton). The total distance form the coil to the plane of calculation is 1.75 cm (compared to 1.7 cm used by Eaton). Because of those two reasons, some differences are expected between the results obtained by the impedance method and those by Eaton.

Fig. 5.8 shows the results obtained by the impedance method. Two plots are shown for the same paths as those of Fig. 5.7 except that only one coil angle (open coil) is used for verification. Some differences are observed. For example, the peak for both plots (a and b) is 185 nV/m while it is 195 nV/m for the corresponding peaks in Fig. 5.7. The percentage difference in the peak value is approximately 5 %. The percentage difference in the coil position and computational plane is $((1.75 - 17)/17) \times 100$ which equals approximatly to 3%. This is a satisfactory result in the sence that a difference of 3% in the distance of the computational plane from the coil results in a difference of about 5% in the value of the electric field. This means that the field calculations using the impedance method is within 2% difference with the results obtained by Eaton. Also, the zero points in Fig. 5.8-a, designated by O_1 and O_2, are not exactly zero, as in Fig. 5.7, this is due to numerical errors. However, the field will approach the zero value at these points if a very fine mesh size is used.

From the discussion above, it is concluded that the code implementing the impedance method works properly and, therefore, it can be used to solve for the induced electric field in more complicated geometries having heterogeneous electrical properties.

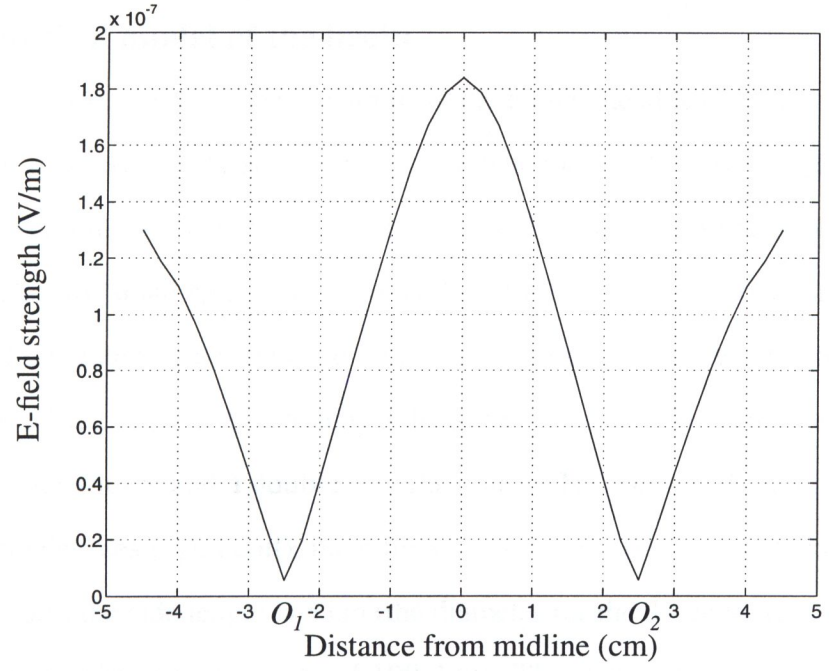

(a)

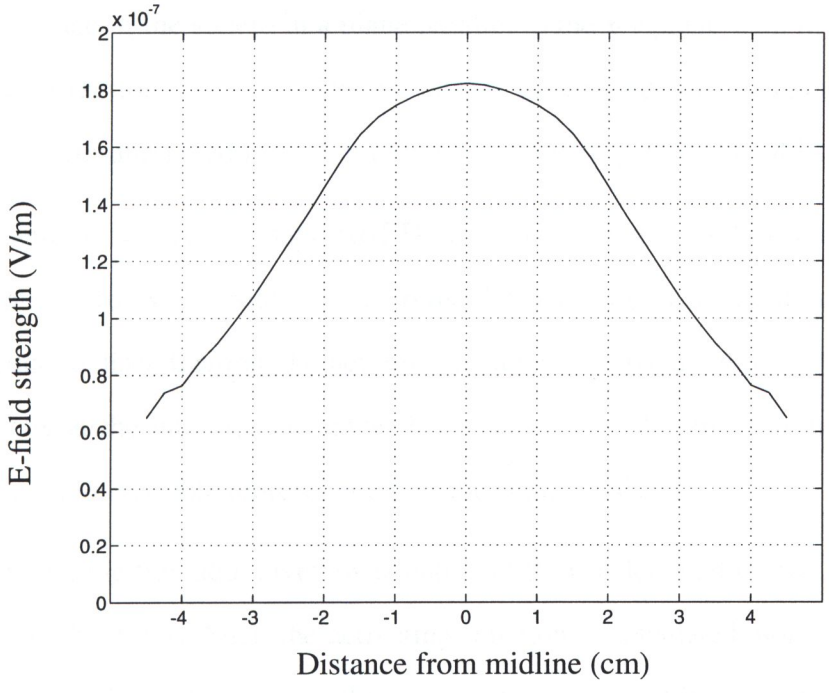

(b)

Figure 5.8 The impedance method calculations of the magnitude of the electric field produced by a butterfly coil with "wing" angle of 180 degrees (open) excited with a current ramp of 1A/s. (a) the field strength along path "a" in a plane 1.25 cm below the sphere surface. (b) The field strength along path "b" in a plane 1.25 cm below the sphere surface.

5.4.2 Spherical model of the brain

In this section stimulation of bent neurons in the human head is investigated. The model of the head is as previously shown in Fig. 5.1. The radius of the outer sphere is R_1 = 9.1 cm and the conductivity is 0.14 S/m [14], the radius of each inner eccentric sphere is 3.75 cm. The two small spheres are evenly displaced with respect to the axis of the outer sphere and separated by a distance d = 0.5 cm. Their conductivity is 0.5 S/m [13]. Their centers are shifted in the z-direction by a distance c = 1.5 cm. Two coil configurations are used, a double-square and a double-circular (butterfly) coil. For both coils, the "wing" angle is 180 degrees (open coil), the number of turns is 10 turns each side (20 turns for the whole coil), the side length is 5 cm (the diameter for the double-circular coil) and carrying a current changing at a rate of 100 A/μs. The stimulating coil is placed 0.5 cm above the surface of the sphere in a plane parallel to the x-y plane with its longer dimention in the y-direction (Fig. 5.3). The previously mentioned coil parameters are typical values for the stimulating coils used in clinical practice (e.g. Cadwell MES-10).

The neuron, having the shape ABCD (as shown in Fig. 5.2), lies in a plane parallel to the x-z plane. To avoid problems due to the discontinuity of the fields at the interfaces and errors due to discretization, the neuron is assumed to have a radius of 4 cm, i.e it does not lie exactly at the interface but rather is displaced by 0.25 cm from the inner sphere. This is not an unreasonable representation of the actual analysis.

The activating function, given by equation (5.9), is calculated in two steps (as previously done in chapter 4). First, the activating function is calculated along the nerve part, BC, for a fixed coil position. Then, the coil position is varied in steps. Five positions of the coil above the nerve are considered. The first position is such that the coil is centered above the outer sphere. In the other positions, the coil is shifted by different amounts in the x-direction (as shown in Fig. 5.9)

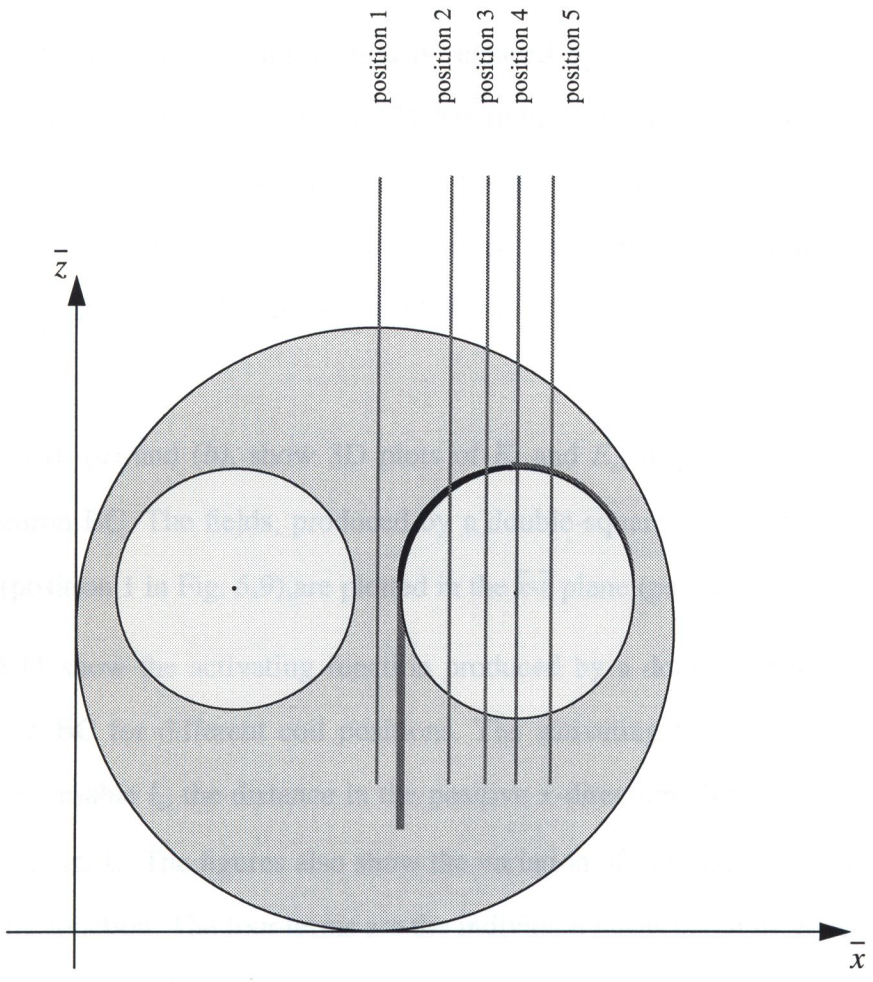

Figure 5.9 Different coil positions. Position 1, the coil center is aligned with the center of the outer sphere. Position 2, the coil is shifted 2 cm in x-direction from position 1. Positions 3-5 are spaced by 1 cm.

Due to discretization, the electric field components, E_x and E_z, are defined at a limited number of points (the number of points equals the number of cells fitted in the region surrounding the neuron, i.e. for 2.5 mm cell size the number of cells is 16). To get more data points, 2D-interpolation (linear) is performed for both E_x and E_z field components. The spatial derivative of both E_x and E_z in the x-direction also need to be obtained (eq. 5.9). Direct numerical differentiation of E_x component, for example, gives a badly behaved function due to the fact that differentiation enhances fine variations (computa-

tional noise) in the function to be differentiated. To avoid this problem a given electric field component after the 2D-interpolation is replaced by the corresponding smoothed component (using the spline method, MATLAB routine "spline"). The electric field is sampled at 8 points and then a spline function is used to fit those points. The resulting field is then differentiated with respect to u (or x). The maximum absolute percentage error in the derivative after using the splined fields is about 8% and the root mean square error is about 1.8%.

Figures 5.10 (*a*) and (*b*), show 3D plots of E_x and E_z, respectively, in the region around the neuron BC. The fields, produced by a double-square coil centered above the outer sphere (position 1 in Fig. 5.9),are plotted in the $\bar{x}$-$\bar{z}$ plane (parallel to x-z plane).

Figs. 5.11 show the activating function produced by a double-circular coil along the bent neuron BC for different coil positions. The activating function is plotted as a function of the variable l_x, the distance in the positive x-direction along the neuron measured from the point C. The figures also show the variation of the four terms contributing to the activating function. The four terms are the individual terms given by equation (5.9). It is noticed from Figs. 5.11 that the maximum value of the activating function increases (in absolute value) and its location shifts toward point B at the neuron when the coil is positioned away from the center or the outer sphere. For example, the maximum value of the activating function for the coil position 1 is -0.1 V/cm^2 and is located 2.23 cm from point B on the nerve, while for the coil position 2 the value is -0.14 V/cm^2 and at 1.68 cm from point B. The activating function reaches its maximum (in absolute value) when the coil is positioned in such a way that its center is directly above the highest point on the nerve (i.e. point B). This position is designated by position 4 in Fig. 5.9. The activating function starts to decrease again when the coil position is changed to position 5. This

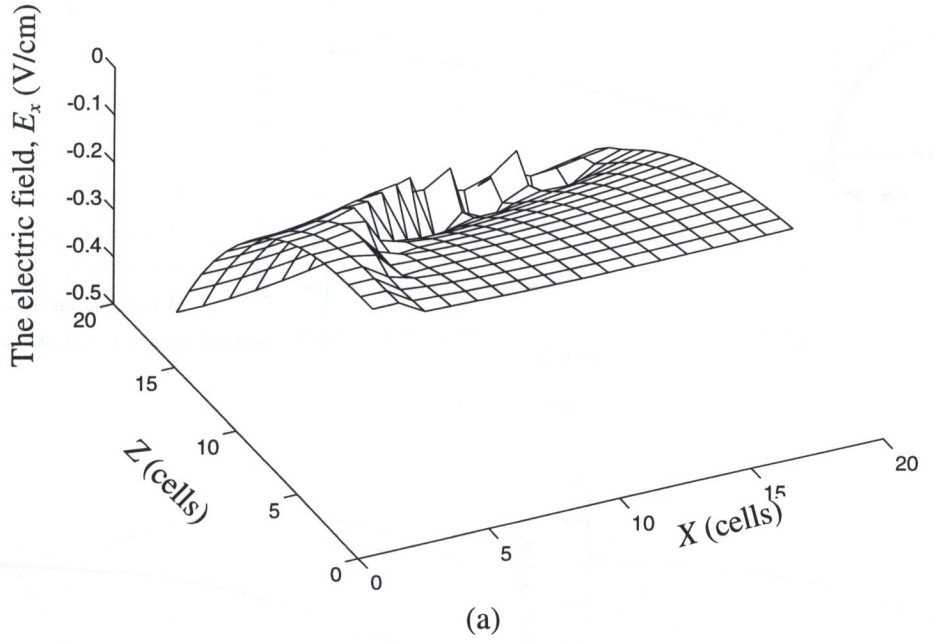

(a)

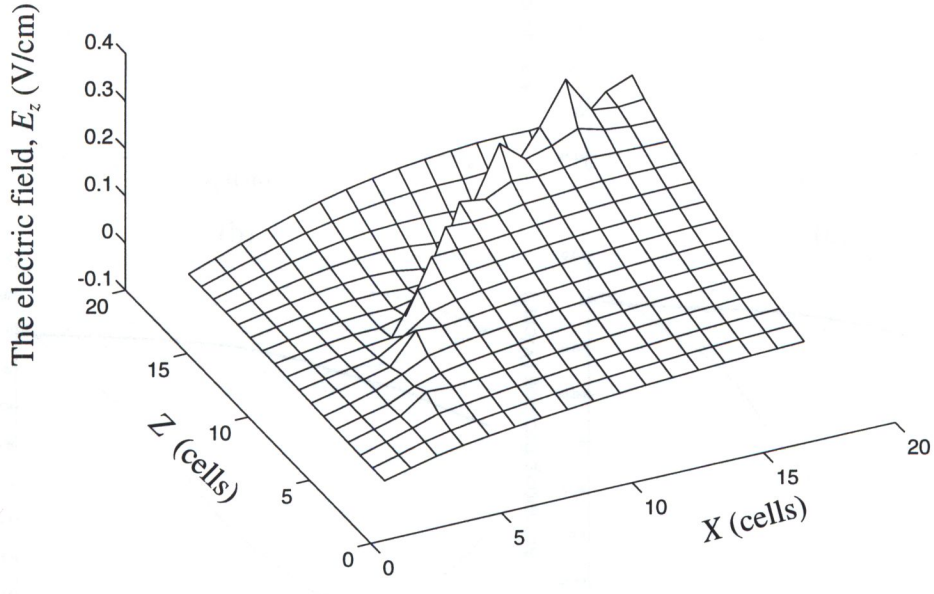

(b)

Figure 5.10 3D plots of the electric field components in a square region surrounding the nerve BC (16x16 cells). (a) The x-component. (b) The z-component.

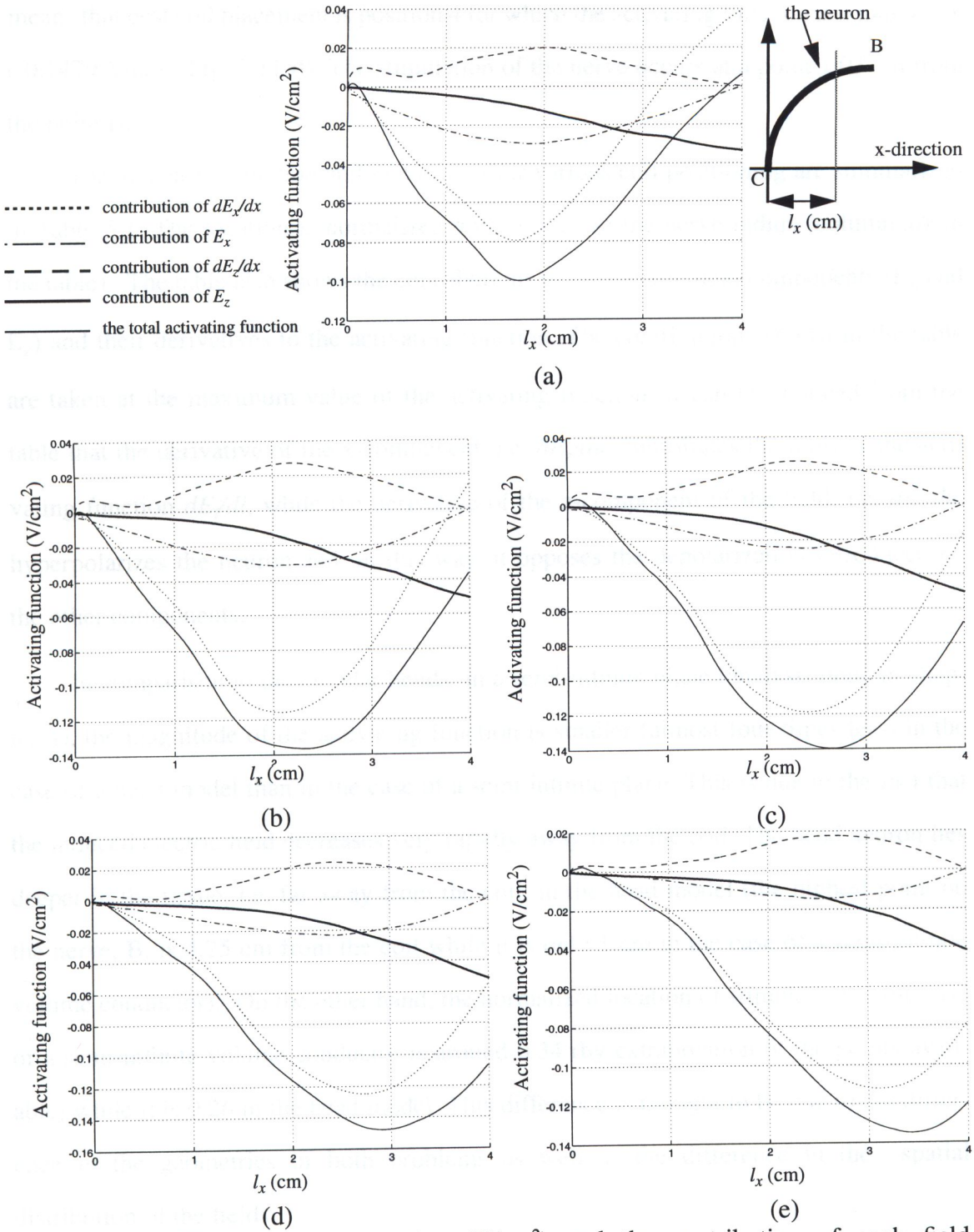

Figure 5.11 The activating function (V/cm^2) and the contribution of each field component and its derivative to it for a double-circular coil of 5 cm diameter (a side), vs. the distance l_x, along the bent neuron for different coil positions: (a) Position 1. (b) Position 2. (c) Position 3. (d) Position 4. (e) Position 5.

means that best coil placement is position 4 for which the activating function is a maximum (-0.1479 V/cm^2, Fig. 5.11-d). The stimulation of the nerve occurs at a point 1.03 cm from the point B.

The activating function and its location for various coil positioning are summarized in Table 5.1. The location is normalized with respect to the nerve radius (column *x/r* in the table). The table also shows the contributions of the electric field components (E_x and E_z) and their derivatives to the activating function. The contributions shown in the table are taken at the maximum value of the activating function. It can be noticed from the table that the derivative of the x-component, i.e. dE_x/du, contributes the most to the activating function dE_f/dl, while the derivative of the z-component of the field, i.e. dE_z/du, hyperpolarizes the neuron and, in this way, it opposes the depolarization introduced by the other components.

In comparison to the circular bends in a semi-infinite plane (analysis done in chapter 4), the magnitude of the activating function is smaller (almost four times less) in the case of a head model than in the case of a semi-infinite plane. This is due to the fact that the induced electric field decreases very rapidly away from the coil. The bend neuron lies deeper in the tissue, i.e. far away from the coil, in the head model (the highest point on the nerve, B, is 4.25 cm from the coil while it is only 1 cm in the case of a semi-infinite volume conductor). On the other hand, the normalized location of stimulation in the case of a semi-infinite volume conductor is around 0.34 (by extrapolation of the points available) while it is 0.26 in the head model. This difference is thought to be due to the difference in the geometries of both problems as well as the difference in the spatial distribution of the fields.

Table 5.1 Activating function and individual contributions. Stimulation to it produced by a double-circular coil of diameter 5 cm, 20 turns (10 turns each side) and carrying current varying at a rate of 100 A/μs

Coil position	Activating Function (V/cm^2)	Individual contributions to the activating function				Location	
		$T_1.dE_x/du$	$T_2.E_x$	$T_3.dE_z/du$	$T_4.E_z$	$(4 - l_x)$(cm)	$(4 - l_x)/r$
Position 1	- 0.100	-0.079	-0.029	+ 0.019	- 0.010	2.23	0.56
Position 2	-0.136	-0.113	-0.031	+ 0.027	- 0.019	1.68	0.42
Position 3	-0.140	-0.116	-0.023	+0.024	-0.024	1.31	0.33
Position 4	-0.148	-0.122	-0.019	+0.021	- 0.027	1.03	0.26
Position 5	- 0.135	- 0.109	- 0.010	+ 0.012	- 0.038	0.58	0.14

Fig. 5.12 shows the same parameters as Fig. 5.11 except for a double-square coil. The maximum activating function (magnitude) is also at the same coil placement as that for a double-circular coil. However, the maximum value is higher for the double-square coil (-0.1607 V/cm^2). This means that the double-square coil is preferable for stimulation of bent neurons in the cortex. This result agrees with that obtained for stimulating straight neurons [1], however it contradicts that obtained in chapter 4 where stimulation of bent neurons in a semi-infinite volume conductor was considered. The location of the stimulation is almost the same as that of the double-circular coil (1.05 cm for point B for the double-square coil and 1.03 cm for the double-circular coil).

Table 5.2 show the same parameters as those shown in Table 5.1, except it is for a double-square coil. The derivative of the x-component of the electric field contributes the most to the activating function while the derivative of the z-component introduces a hyperpolarization effect which acts to decrease the activating function.

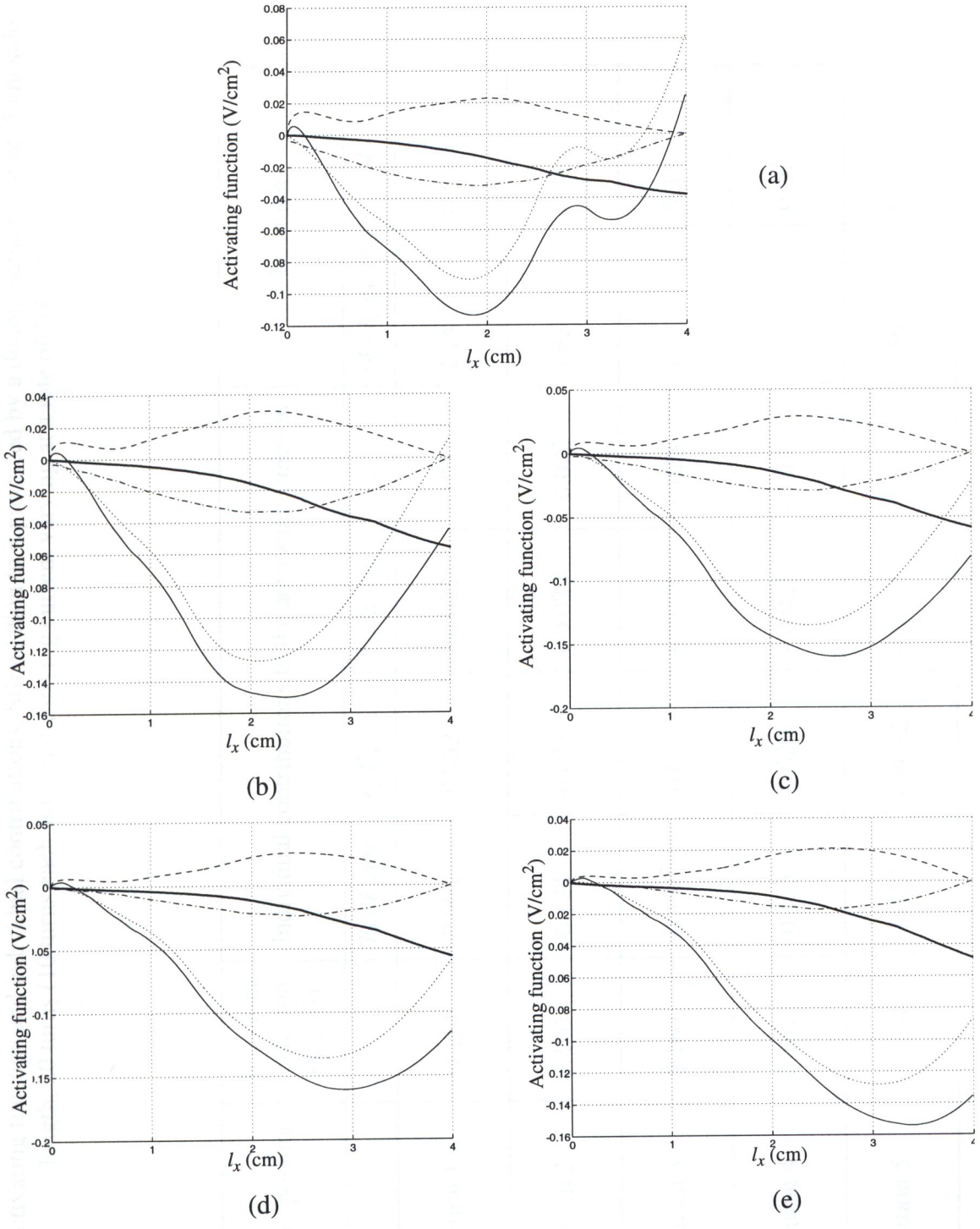

Figure 5.12 The activating function (V/cm^2) and the contribution of each field component and its derivative to it for a double-square coil of 5 cm (a side), vs. the distance l_x, along the bent neuron for different coil positions: (a) Position 1. (b) Position 2. (c) Position 3. (d) Position 4. (e) Position 5.

Table 5.2 Activating function and individual contributions. Stimulation to it produced by a double-square coil of 5 cm side length, 20 turns (10 turns each side) and carrying current varying at a rate of 100 A/μs

Coil position	Activating Function (V/cm^2)	Individual contributions to the activating function				Location	
		$T_1.dE_x/du$	$T_2.E_x$	$T_3.dE_z/du$	$T_4.E_z$	$(4 - l_x)$(cm)	$(4 - l_x)/r$
Position 1	- 0.114	-0.091	-0.032	+ 0.022	- 0.013	2.14	0.53
Position 2	-0.150	-0.124	-0.033	+ 0.029	- 0.022	1.63	0.41
Position 3	-0.160	-0.131	-0.027	+ 0.026	-0.028	1.31	0.33
Position 4	-0.161	-0.133	-0.020	+ 0.023	- 0.030	1.05	0.26
Position 5	- 0.154	- 0.123	- 0.012	+ 0.014	- 0.033	0.59	0.15

5.5 Discussion and conclusions

In this chapter, magnetic stimulation of bent neurons in the human cortex has been analyzed. The head has been modeled as a sphere of radius 9.1 cm and conductivity of 0.14 S/m while the cortex (brain) has been modeled as two spheres, each representing one side of the brain, of radius 3.75 cm and conductivity of 0.5 S/m. The neuron, ABCD, has been considered to have a circular bend of radius 4 cm. Two coil configurations have been used for magnetic stimulation: a double-circular and a double-square coils carrying a current changing at a rate of 100 A/μs. The 3D impedance method has been used to compute the electric field components that contribute to the neuron stimulation, i.e. the x- and z-components.

It has been found that the magnitude of the activating function varies with the position of the coil relative to the neuron. The best coil placement is such that its center is directly over the highest point on the neuron, i.e. point B. This is true for both coil configurations used. However, the magnitude of the activating function is higher when the double-square coil is used. This means that to stimulate (bent) neurons in the human cortex the double-square coil is preferable to the double-circular coil. This result agrees with the results reported for long straight neurons [1].

It is interesting to notice that the double-circular coil produces a higher stimulus than the double-square coil when stimulating bent neurons in the simplified model (the semi-infinite volume conductor with a planar interface) while the latter produces a higher stimulus than the former when studying the stimulation bent neurons in the human head model. Most of the parameters affecting the magnitude and the location of the stimulation are fixed for both coils except two. The first is the coil shape (or geometry), and the second is the coil proximity to the nerve. For long straight neurons double-square coils produce higher stimulus than double-circular coils[1]. On the other hand, for bent neu-

rons, two components contribute to the activating function. The first component is solely dependent on the coil geometry, and the second component results from the interaction between the field produced by the coil and the shape of the neuron bend. The second component is higher for circular coils than for square coils as the former have smooth shape while the latter have sharp corners. When calculating the activating function for bent neurons in a semi-infinite volume conductor model, coils were close enough to the neuron (the coil is positioned 2 cm from the nerve) that the interaction between the coil and the bend is dominating the component depending on the coil itself. This causes the circular coil to have a higher stimulus. On the other hand, for studying the stimulation of bent neurons in the model of the human head, the stimulating coil was farther away from the bend (4.5 cm) than in the case of a semi-infinite conductor. Accordingly, the component due to the coil itself dominates the component due to the coil-bend interaction and the double-square coil in this case has a stronger stimulus than the double-circular coil.

The location of the stimulation is more or less the same for both coil configurations and it is about 1 cm from the point B (the highest point on the nerve) in the direction of the center of the larger sphere. The normalized location of stimulation is somewhat different for the bent neuron in the head from that in a semi-infinite volume conductor. However, both cases agree in the sense that the stimulation is closer to the point on the nerve where the slope with respect to the u-axis (or x-axis) is zero (point B) than that of an infinite slope (point C).

Some errors are associated with this analysis. The first error is the discretization error. The FD approximation of Maxwell's equation neglects the higher order derivatives and assumes that the fields are uniform within each computational volume. Also, when the geometry is discretized, it loses some of its properties. For example, the sphere after discretization is not a perfect sphere. Therefore when we assign electrical properties to

the different cells we might assign an air cell while part of the cell is actually conducting. Actually, after discretization the solution is obtained for a system that only approximates the actual system. Also, when calculating the EMF for each loop in the circuit mesh representing the biological body, the magnetic field is considered constant while in reality it is varying across the plane of the loop.

Discretization errors can be minimized by using a fine grid (smaller cell dimensions), especially at the interfaces. In practice, there is always a compromise between the accuracy on one hand, and the computation time and computer memory and storage on the other hand.

A second source of error is due to the assumption that the neuron is located one cell outside the small sphere. This error can also be minimized by using smaller cell sizes.

A third error is due to the 2D-interpolation of the electric fields. However, using the values of the fields before interpolation will result in larger errors as the number of points is limited to only 16.

Obtaining the derivatives of the fields by sampling them at a limited number of points and producing a smoother fields using the spline method then differentiating, is a fourth source of error. The error in the derivative is maximum 8%, and a root-mean-square (RMS) is 1.8%. This error is not serious as the RMS error is less than 2%.

This analysis is valid whenever the quasi-static condition is valid, i.e. within the frequency limit given by equation (5.14).

Chapter 6

Conclusions and recommendations

6.1 Conclusions

Neuron stimulation by external stimulators is widely used as a diagnosing tool for several neuron disorders. It is realized either by external electrodes (electrical stimulation) or coils carrying time varying currents (magnetic stimulation). Magnetic stimulation is considered as an alternative to electric stimulation because it is a painless and non-invasive.

The activating function (stimulus) is the spatial derivative of the electric field along the neuron. Its magnitude and the location of the stimulation are the important parameters in neuron stimulation. For peripheral neuron stimulation, the neuron is modeled as being **long and straight**. This assumption is also valid for terminated neurons as long as the termination is far from the stimulating coil. In this case, the magnitude and the location of the stimulus depend on the coil position and configuration.

Different coil configurations were used for magnetic neuron stimulation. Circular, square, double-circular (butterfly), double-square and the quadruple-square coils. Time varying currents can be either monophasic (ramp, or pulse) or biphasic (sinusoidal). The time variation of the coil current is such that its maximum frequency component is within the **quasi-static** limits of 10 kHz.

Stimulating motor neurons in the human cortex where they are bent, the activating

function is found to be a function of both the coil configuration and the **bend shape**. A simplified analysis considered the activating function of a straight neuron with a bend in a semi-infinite volume conductor of a planar interface (chapter 4). In this case, both the electric field in the direction of the straight part of the neuron and its derivative contribute to the activating function of the neuron. Two coil configurations (double-square and double-circular coils) as well as different bend shapes (a cosh, a parabolic, and circular bends of different radii) were considered. The results show that the maximum stimulation occurs on the bent part of the neuron. The stimulation threshold is the lowest for the greatest curvature of the nerve. For instance, for the circular bends, it is the lowest for the smallest radius analyzed (1 cm). This result is in excellent agreement (qualitatively) with the experimental results reported by Maccabee et al. [4]. The analysis also showed that the double-circular coil produced a higher stimulus than the double-square coil of comparable dimensions. This result is contrary to that obtained for straight neurons [1].

A more realistic analysis considers stimulating a bent neuron in the human cortex (chapter 5). The head is modeled as an outer sphere representing the skull and scalp with two spheres inside, each representing one half of the brain. The neuron consists of two parts: a straight part, and a bent part (circular of radius 4 cm). Two coil configurations used are: a double-circular and a double square coils.

The analysis shows that the activating function varies with the coil position with respect to the nerve. For both coil configurations, the optimal position is such that the coil center is directly over the highest point of the nerve (point B, Fig. 5.2-a) and the location of the stimulation is found to be closer to point B than point C (Fig. 5.2-a). This result agrees with that obtained for the same bend in a semi-infinite volume conductor. The results also show that the double-square coil produces a higher activating function than the double-circular coil of comparable dimensions. This means that this is the pre-

2- The head model:

A more realistic model of the head that takes into account the exact shape of the brain and the irregularities of the skull and scalp needs to be considered. Such a model takes into account the existence of other tissues in the cortex (e.g. the cerebellar cortex). This model can be obtained using digitized magnetic resonance imaging (MRI) of the head. Then using image processing, a 3D-model of the head can be constructed with different conductivities assigned to different biological tissues in the model. Developing this model depends on the available image processing tools. Also, the construction of the 3D-model from the MRI slices is considered a big challenge in the field of image processing.

3- The nerve model:

It is not always the case that the neuron lies in one plane but rather it can assume a 3D-shape. In this case, field components in all directions contribute to the neuron stimulation and each of them is a function of two dimensions (they are functions of only one dimension for a planar neuron). The activating function has to be recalculated, and a more complicated form is expected. However, this model is more realistic than the planar model, and more accurate results (in terms of the location and magnitude of the activating function) can be obtained.

If the neuron is terminated and the termination is close to the coil position, the activating function has to be derived from the cable model of the neuron considering its termination. This is a different and fairly complicated problem of magnetic stimulation but it is thought that its analysis is of importance as most of the neurons in the human head are terminal neurons.

Bibliography

[1] K..P. Esselle and M.A. Stuchly, "Neural stimulation with magnetic fields: analysis of induced electric field", *IEEE Trans. Biomed. Engineering*, vol. 39, pp. 693-700, 1992.

[2] T. H. H. G. Koh, and J. A. Ayre, "Maturation of corticospinal tracts assessed by electromagnetic stimulation of the motor cortex", Arch. Dis. Child., vol 36, 1988.

[3] M. A. Stuchly, "Applications of time-varying magnetic fields in medicine", Clinical Review in Biomedical Engineering, vol. 18, issue 2, pp. 89-124, 1990.

[4] P. J. Maccabee, V. E. Amassian, L. P. Eberle, and R. Q. Cracco, "Magnetic coil stimulation of straight and bent amphibian and mammalian peripheral nerve *in vitro*: locus of excitation", *J. of Physiol.*, vol. 460, pp. 201-219, 1993.

[5] P. J. Basser, R. S. Wijesinghe and B. J. Roth, "The activating function for magnetic stimulation derived from a three-dimensional volume conductor model", *IEEE Trans. Biomed. Eng.*, vol. 39, pp. 1207-1211, 1992.

[6] P. J. Basser and B. J. Roth, "Stimulation of a myelinated nerve axon by electromagnetic induction", *Med. & Biol. Eng. & Comput.*, vol. 29, pp. 261-268, 1991.

[7] A. T. Barker, R. Jalinous and I. L. Freeston, "Non-invasive magnetic stimulation of human motor cortex," Lancet, i:1101-1107, 1985.

[8] L. G. Cohn, S. Bandinelli, S. Lelli and M. Hallett, "Non-invasive mapping of head motor somatotopic area using magnetic stimulation," Clin. Neurophysiol., vol. 5, pp. 371-372, 1988.

[9] A. T. Barker, I. L. Freeston, R. Jalinous and J. A. Jarratt, "Magnetic stimulation of the human brain and peripheral nervous system: an introduction and the results of an initial clinical evaluation," Neurosurgery, vol. 20, pp. 100-109, 1987.

[10] L. G. Cohen, B. J. Roth, J. Nilsson, N. Dang, M. Panizza, S. Bandinelli, W. Friauf and M. Hallett, "Effects of coil design on delivery of focal magnetic stimulation, Technical consideration", Electroenceph. clin. Neurophysiol., 1989.

[11] P. S. Tofts, "The distribution of induced currents in magnetic stimulation of the nervous system," Phys. Med. Biol., vol. 35, pp 1119-1128, 1990.

[12] S. Ueno, T. Matsuda and K. Harada, "Localized stimulation of neural tissues in the brain by means of a paired configuration of time-varying magnetic fields," Appl. Phys., vol. 64, pp. 5862-5864, 1988.

[13] B. J. Roth, J. M. Saypol, M. Hallett, and L.G. Cohen, "A theoretical calculation of the electric field induced in the cortex during magnetic stimulation", *Electroencephal. Clin. Neurophysiol.*, vol. 81, pp. 47-56, 1991.

[14] H. Eaton, "The electric field induced in a spherical volume conductor from arbitrary coil: Application to magnetic stimulation and MEG," Med. Biol. Eng. Comp., vol.30 pp. 433-440, 1992.

[15] A. P. Spence, *Basic human anatomy*, Redwood city, CA: Benjamin/Cummings, 1990

[16] R. Plonsey, *Bioelectric phenomena*, New York, NY: Mcgraw-Hill, 1969.

[17] J. Patrick, "Electrical model for neural excitation studies", Johns Hopkins APL Technical Digest, vol. 9, no. 1, pp. 44-59, 1988.

[18] R. Plonsey and R. C. Barr, *Bioelectricity: A quantitative approach*, Plenum Press, N.Y., 1988

[19] B. J. Roth, P. J. Basser, "A model of the stimulation of a nerve fiber by electromagnetic induction," IEEE Trans. Biomed. Eng. vol. 37, pp. 588-597, 1990.

[20] F. Pattay, "Modeling the excitation of fibers under surface electrodes", IEEE Trans. Biomed. Eng. vol. 35, no. 3, pp. 199-203, 1988.

[21] P. A. Merton, and H. B. Morton, "Stimulation of the cereberal cortex in the intact human sbjects," Nature, 285:227, 1980.

[22] P. A. Merton, H. B. Morton, D. K. Hill, and C. D. Marsden,"Scope of a technique for electrical stimulation of human brain, spinal cord, and muscle", Lancet, vol. 2, pp. 597-600, 1982.

[23] M. Polson, A. T. Barker, I. L. Freeston, "Stimultion of nerve trunks with time-varying magnetic fields", Med. Biol. Eng. Comut., vol 20, pp. 243-244, 1982.

[24] A. T. Barker, I. L. Freeston, R. Jalinous, J. A. Jarrat, "Motor responses to non-invasive brain stimulation in clinical practice", Electroencephal. Clin. Neurophysiol. 1985 :S70.

[25] A. d'Arsonval, "Dispositifs pour lameasure des courants alternatifs de toutes frequences", CR Soc Biol (Paris) 1896; May 2:450-1.

[26] A. Kolin, N. Q. Brill, P. J. Broberg, "Stimulation of irritable tissue by means of an alternating magnetic field", Proc. Soc. Exp. Biol. Med. 1959; 102:251-3

[27] R. G. Bickford, B. D. Fremming, "Neural Stimulation by Pulsed magnetic fields in animals and man", Digest of the 6th International conference on medical electronics and biological Engineering, 1965 (Tokyo), paper 7-6.

[28] A. M. Portis, *Electromagnetic fields: Sources and Media*, New York: John Wiley & Sons, Inc., 1978.

[29] F. X. Hart, *Mathematical modeling of electromagnetic interactions with biological systems. in: Modern Bioelectricity*, A. A. Marino, Ed. MArcel Dekker, New York, NY, pp. 281-344, 1988.

[30] R. S. Elliott, W. H. Harrison and F. K. storm, "Hyperthermia: electromagnetic heating of deep-seated tumors", IEEE Trans. Biomed. Eng., vol. 29, pp. 61-64, 1892.

[31] S. C. Hill, D. A. Christensen and C. H. Durney, "Power deposition in magnetically induced hyperthermia: A two-dimentional low-frequency numerical analysis", Int. Radiation Oncology Bio. Phys., vol. 9, pp. 893-904, 1983.

[32] D. W. Armitage, H. H. Le Veen, and R. Pethig, "Radiofrequency-induced hyperthermia: computer simulation of specific absorption rate distributions using realistic anatomical models", Phys. Med. Biol., vol. 28, pp. 31-42, 1983.

[33] R. Plonsey, and D. Heppner, "Considerations of quasi-stationarity in electrophysiological systems", Bull. Math. Biophys., vol. 29, pp. 657-664, 1967.

[34] H. P. Schwan, C. F. Kay, "The conductivity of living tissues," Ann. NY Acad. Sci:, vol. 65, pp. 1007-1013, 1956.

[35] R. Antolini, G. Cerri, L. Cristoforetti and R. DeLeo, "Absorbed power distributions from single or multiple waveguide applicators during microwave hyperthermia", Phys. Med. Biol., vol. 31, pp. 1005-1019, 1986.

[36] D. M. Sullivan, D. T. Broup and O. P. Gandhi, "Use of the finite-difference time-domain method in calculating EM absoption in human tissues", IEEE Trans Biomed. Eng., vol. 34, pp. 148-157, 1987.

[37] J. Y. Chen and O. P. Gandhi, "RF currents induced in an anatomically-based model of a human for plane-wave exposures (20-100 Mhz)", Health Physics, vol. 57, pp. 89-88, 1989.

[38] M. Guidi, O. Scrpino, F. Angeleri, R. Antili and R. De Leo, "Brain cortex stimulation by using magnetic pulses: Analysis of induced current distribution by means of a computer simulated model", IEEE Eng. Med. Biol. Soc. 11th Annual International Conference, Seattle, WQ, pp. 1169-1171, 1989.

[39] K. R. Foster, and H. P. Schwan, "Dielectric properties of tissues and biological materials: A critical review", CRC Crit. Rev. Biomed. Eng., vol. 17, pp. 25-104, 1989.

[40] B. J. Roth, L. G. Cohen, M. Hallett, W. Friauf, and P.J. Basser, "A theoretical calculation of the electric field induced by magnetic stimulation of a peripheral nerve", *Muscle & Nerve*, vol. 13, pp. 734-741, 1990.

[41] F. Grandori and P. Ravazzani, "Magnetic stimulation of motor cortex-Theoretical considerations," IEEE Trans. Biomed. Eng., vol. 38, pp. 180-191, 1991.

[42] N. M. Branston and P. S. Tofts, "Analysis of the distribution of currents induced by a changing magnetic field in a volume conductor,"Phys. Med. Biol., vol. 36, pp. 161-168, 1991.

[43] P. J. Maccabee, V. E. Amassian, R. Q. Cracco, J. A. Cadwell, "An analysis of pereferal motor nerve stimulation in humans using the magnetic coil," Electroenceph. Clin Neurophysiol., vol. 70, pp. 524-533, 1988.

[44] G. D'Inzeo, C. Giacomozzi, and S. Pisa, "Analysis of the stimulation of a nerve fiber surrounded by an inhomogeneous, anisotropic, and dispersive tissue," Applied Computational Electromagnetics Socity, vol. 7, no. 2, pp. 179-190, 1992.

[45] K. P. Esselle, and M. A. Stuchly, "Quasi-Static electric field in a cylinderical volume conductor induced by external coils," IEEE Trans. Biomed. Eng., vol. 41, no. 2, pp. 151-158, 1994.

[46] D. Cohen and B. N. Cuffen, "Developing a more focal magnetic stimulator- Part I: somebasic principles," J. Clin. Neurohpysiology, vol. 8, pp. 102-111, 1991.

[47] S. Rush and D. A. Driscoll, "Current distribution in the brain forn surface electrode," Anesth. Analg., vol. 47, pp. 717-723, 1968.

[48] S. Rush and D. A. Driscoll, "EEG electrode sensitivity-An application of receprocity," IEEE Trans. Biomed. Eng., vol. 16, pp. 15-22, 1969.

[49] B. N. Cuffin, "Eccentric spheres model of the head," IEEE Trans. Biomed. Eng. vol. 38, pp. 871-878, 1991.

[50] J. P. Reilly, "Pereferal nerve stimulation by induced electric currents: exposure to time-varying magnetic fields", Med. & Biol. Eng. & Comput., vol. 27, pp. 101-110, 1989.

[51] S. Ueno, T. Matsuda, and M. Fujiki,"Functional mapping of the human cortex obtained by focal and vectroial magnetic stimulation of the brain," IEEE Trans. Mag., vol. 26, pp. 1539-1544, 1990.

[52] P. Silvister, *Modern electromagnetic fields*, Englwood cliffs, N.J.: Printice-Hall, 1968.

[53] K.P. Esselle and M.A. Stuchly, "Simplified analytical solutions for magnetic stimulation of neurons", *Applied Comput. Electrom. Soc. J.*,vol. 7, pp. 162-178, 1992.

[54] W. Xi, M. A. Stuchly and O. P. Gandhi, "Induced electric currents in models of man and rodents from 60 Hz magnetic fields," IEEE trans. Biomedical Engineering, vol. 14 (in press) 1994.

[55] M. A. Stuchly and W. Xi, "Modeling induced currents in biological cells exposed to low-frequency magnetic fields," Phys. Med. Biol., vol. 39, pp. 1319-1330, 1994.

[56] C. Polk, "Electric fields and surface charges induced by ELF magnetic fields," Bioelectromagnetics, vol. 11, pp. 189-201, 1990.

[57] J. F. Deford and O.P. Gandhi, "An impeadance method to calculate currents induced in biological bodies exposed to quasi-static electromagnetic fields," IEEE Trans. Electromagn. Comput. EMC, vol. 27, pp. 168-173, 1985.